Advanced Solar-hybrid Adsorption Cooling System for Decentralized Storage of Agricultural Products in India
— Final Report Phase 1 —

This project is supported by the European Commission (DG XII)

Project No.: ERB3501PL931043IN

DLR

DLR, Institute of Technical Thermodynamics
Stuttgart, Germany
Kai Oertel, Uwe Sprengel

teri

TERI New Delhi, India
Sanjay Mande, V.V.N.Kishore, Pradyumna Ghosh

October 1996

Contents

List of Figures

List of Tables

Chapter 1

Introduction

1.1 Preamble

In a tropical country like India the importance of refrigeration can hardly be overemphasized. Agricultural products play a significant role and could yield substantial foreign trade for the country. However, between production and actual sales about 30% of the produce is spoiled in storage and transit. This alarmingly high spoilage rate calls for closer attention to efficient methods of storage.

The most important method used for preventing spoilage is preservation in cold storage. In 1947, there were only 4 cold storage units in India while in 1972 there were 1990 and there are more than 2500 today. This continual increase in storage capacity is still dwarfed by the growth in production of cold storage items like eggs, vegetables, fish, diary products, etc.. In most Indian cold storages temperatures ranging between -1°C and 10°C are required. Beside this there is also a smaller demand for freezing at temperatures of -18°C and -10°C, e.g. for conservation of meat.

Indian food production centers are usually situated in areas where the electrical power supply for the operation of conventional refrigeration plants is either not available or is not reliable. Refrigeration plants driven by renewable energy sources represents an attractive alternative.

The electrical grid is not very reliable in India, due to frequent power cuts. Therefore even at places where electricity is available from the grid, a sorption refrigeration system, which utilizes maximum energy in thermal form and very little in electrical form for its operation could be most suitable, to disburden the grid. Furthermore the food production centers in rural regions are most convenient for harnessing solar energy over vast open areas.

1.2 Project objectives

The central objective of the project is to provide a cold storage system that meets the needs of the rural food production in India.

The demand for the cooling of agricultural products is generally a growing in India . The major application for food cold storage is the cooling of potatoes. The intended storage of potatoes requires cold store temperatures of about 1-3°C, and thus brine temperatures have to be below or close to 0°C.

It is planned to operate a storage for potatoes by an adsorption cooling system driven by solar collectors and a wood gas (producer gas) boiler as backup system. The driving temperature therefore should be limited to 90°C.

A major problem is that a suitable refrigeration system is not available on the market. The commercially available sorption cooling systems either need driving temperatures above 120°C or cannot reach cooling temperatures below 0°C.

The overriding objective of this two phase project is to study, design, develop, test and to demonstrate *an advanced solar hybrid adsorption cooling system for the decentralized storage of agricultural products in India.* Such a system could later be applied on a large scale and can be produced by the Indian industry.

The major tasks of phase 1 are:

- preliminary design of a technical reference system
- test of different components
- development of a computer model for a solar hybrid adsorption cooling system
- simulation of the system performance
- study on the effect of different operating and design parameters
- elaboration of the techno-economic feasibility of the system under different conditions
- final design of a test plant

These tasks are worked out jointly by TERI and DLR. TERI is mainly in charge of the evaluation of the local conditions, the biomass gasifier technology and techno-economic feasibility study. DLR concentrates on the the system simulation and the component research on the adsorption cooling system.

Chapter 2

Meteo-data and Load-profile

2.1 Evaluation of meteo-data

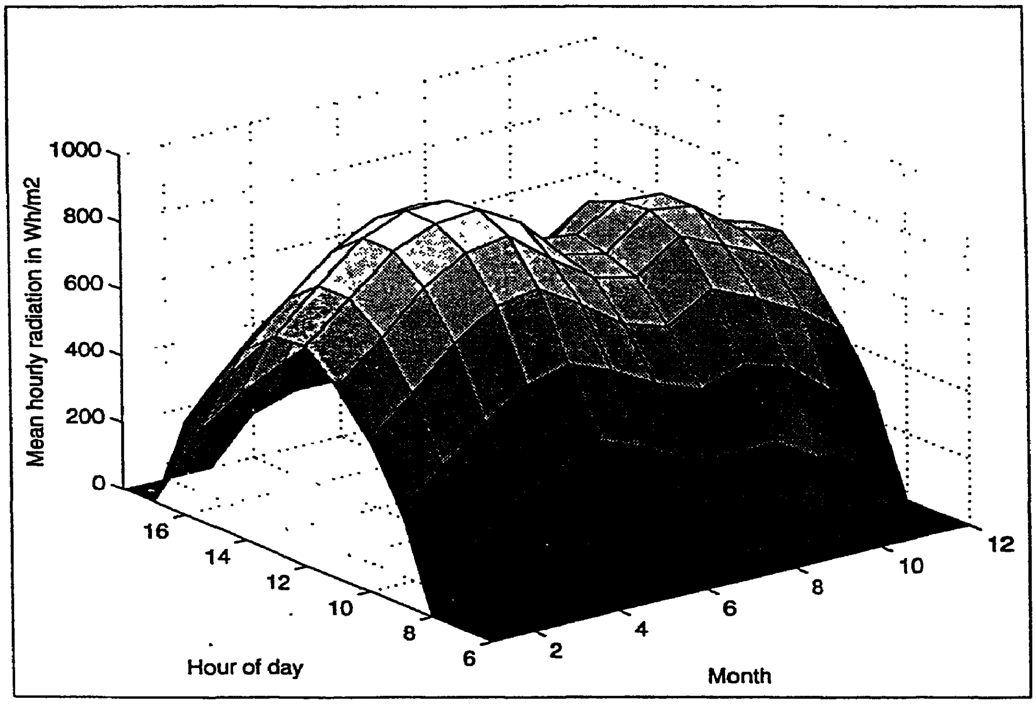


Figure 2.1: Global solar radiation for New Delhi [10]

From the Indian Meteorological Department hourly temperature data for one complete calendar year are obtained for New Delhi, containing direct normal radiation, total horizontal radiation, ambient temperature and relative humidity. Additionally monthly averages of these values and the wind speed are available.

For the solar part normal radiation and ambient temperature are of importance. For the evaluation of the cooling load also the relative humidity has great influence.

2.1.1 Solar radiation

Geographically India is situated between latitude 8°N and 36°N and longitude 62°E and 96°E. It has certain parts that experience extreme conditions of climate. During the year as a whole, more than 2000 kWh/m^2, are received over states of Rajastan and Gujarat, with 3000 to 3200 hours of bright sunshine, while states of East-Bihar, West Bengal and Assam receive less than 1700 kWh/m^2. the annual average of solar radiation intensity for India is 5.7 kWh/m^{2}day and even in the month of December the value is around 5.3 kWh/m^{2}day for some parts of India. For the design of the cold store the weather data of New Delhi are chosen, as there is a great potato framing are close to Delhi, where the cold store could be operated. Fig. 2.1 gives mean values of hourly solar radiation for New Delhi according to Mani[10].

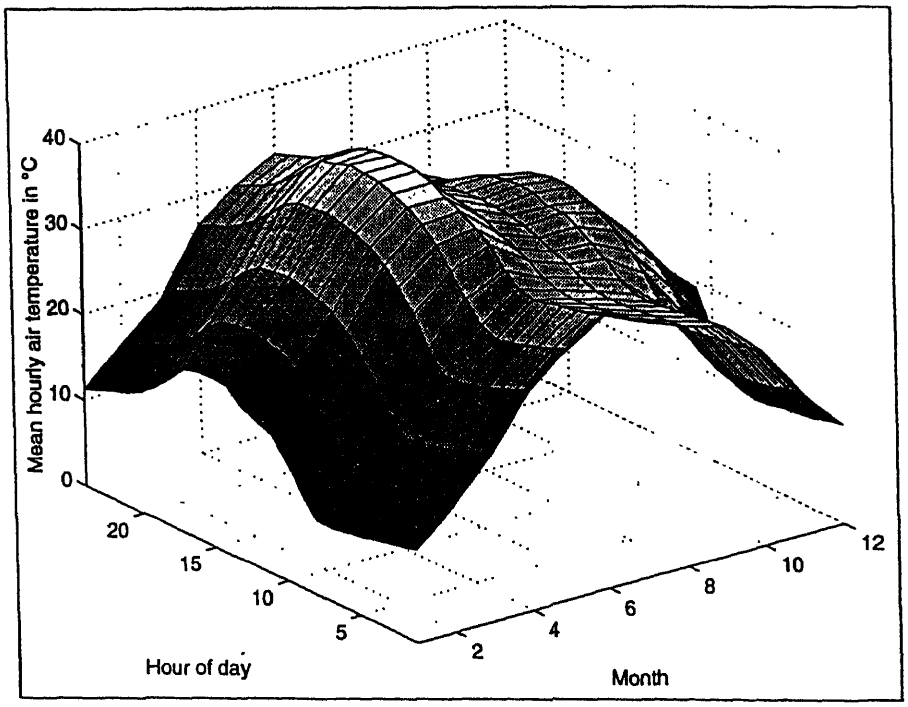


Figure 2.2: Ambient temperature for New Delhi [9]

2.1.2 Ambient temperature

The load for cold storages is mainly determined by the ambient temperature. Fig. 2.2 gives the values for New Delhi. Here temperature ranges between 8.6 (in January) to 38.7 °C (in May) with daily temperature swings of about 7-12 K.

2.1.3 Relative humidity

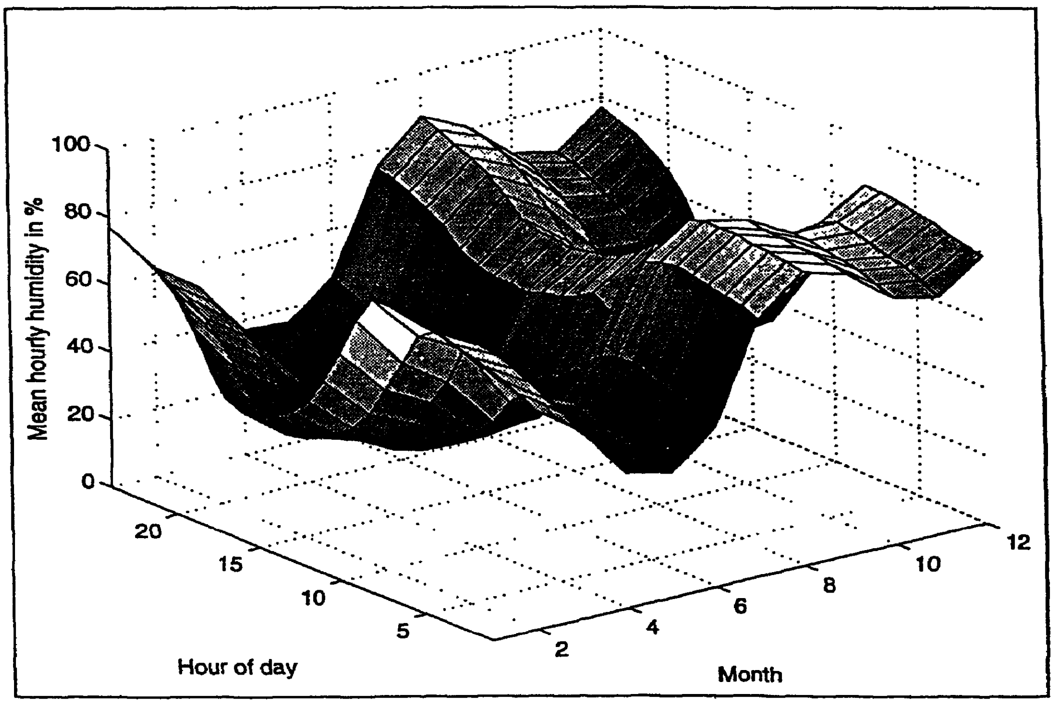


Figure 2.3: Mean hourly humidity for New Delhi [9]

Due to the wet season with lots of rain there is a peak of 90% relatively humidity in August in spite of the high ambient temperatures. Beside this there is also a relatively high humidity in the early mornings of January, when ambient temperature cools down and thus causes relatively high humidity. Both peaks however are no major problems, as this humidity peaks don't match with the temperature peak in April, where humidity with 20-30% is quite low.

2.2 Evaluation of load-profile

2.2.1 Cold storage in India

Presently there are more than 2500 cold storages distributed all over India. Even though cooperative movement is strong in rural areas, majority of the cold storage are in the private sector. The distribution of cold storage among different sectors is given in Tab. 2.1[4].

Sector	Numbers	%	Tons	%
Private	2146	85.0	4652640	91.2
cooperative-operative	188	7.5	351471	6.9
Public	188	7.5	94996	1.9
Total	2522	100.0	5099115	100.0

Table 2.1: Sector-wise distribution of cold storage in India

During the information collection and survey of cold storages it was observed that the maximum number of cold storages are located in rural or semi-urban areas. Potato cold storages contribute to the major share with more than 85%. This finding was different than common belief that maximum cold storage may be storing items like meat, milk products and fruits. In urban areas cold storages are generally used round the year for storing more than one commodities.

2.2.2 Potato cold storages

As said earlier potato cold storage constitutes major share both in numbers as well as storage capacity. Majority of the potato cold storages are located in rural or semi-urban areas. They are generally used exclusively for potatoes. The total annual production of potato in India is about 35 million tons. Thus it can be observed that still only 12-13% of total potatoes are stored in cold storage, indicating the vast potential for growth in potato cold storage in future. Uttar Pradesh (North India) takes the lead in potato production (more than 70%) and so obviously it has major share in number of potato cold storage in India. Since it is closer to Delhi, survey of cold storage was carried out in Delhi as well as Hapur and Ghaziabad region of Uttar Pradesh for collecting detail information about existing potato cold storages.

2.2.3 Survey of potato cold storages in Uttar Pradesh

Common general information is summarized below:

- These storages are exclusively used for potato storage.
- Generally the temperature maintained inside cold storage is about 1 to 1.5°C.
- The potato loading season is from mid February to end of March or at the most till first week of April.
- Potato storage is closed down in November or in small capacity storage even by October end and later on cleaned and made ready for next season which starts in following February.
- Therefore during February and March compressors operate almost continuously for 20-24 hrs.
- The compressor operation duration gradually decreases as cold storage achieves stable temperatures inside (1-2.2°C) to 12-16 hrs in April-May 16-18 hrs in June-July and than reduces from mid August onward and becomes 6-8 hrs in October - November as quantity of potato stored decreases.
- Power supply in such semi-urban areas (as well as even in Delhi where maximum cold storages are located) is not reliable. Many cold storages have diesel genset (100-200 kW capacity depending upon the size of the cold storage) to operate the vapor compression refrigeration system.

2.3 Cooling load profile of potato cold storage

In order to design an alternative solar-hybrid refrigeration system, the first thing required is to find out the cooling load profile which it has to support. In order to get an idea of the cooling load profile of the existing cold storage, information was collected through field survey of few selected units. Due to lack of sophisticated control mechanism, presently the cold storage compressor operation is carried out manually, i.e. the switching on and off of the compressor is not done automatically through inside temperature sensors, but instead typical on-off schedule is adopted by individual cold storage operator through long experience and depending upon load shedding in respective regions. Therefore to get an insight into the average cooling load information about compressor capacity and its on-off time duration in different seasons was collected at selected cold storages.

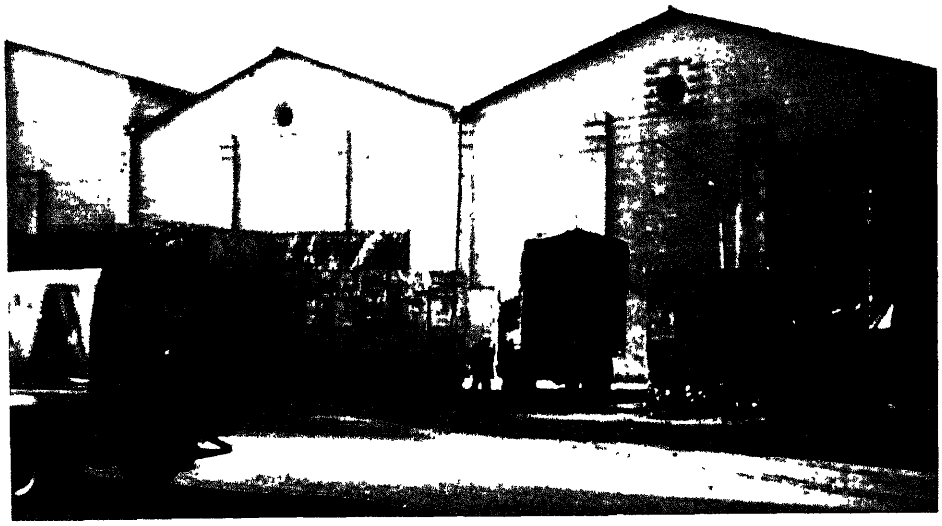


Figure 2.4: GOPI potato cold storage, Hapur (7200 MT capacity)

Comparing the values of the running averages of the measured cooling load in Fig. 2.5 with the profile of the daily ambient temperature, it can be observed that the time of compressor operation and load on the cold storage do not match. The reason for this deviation is, that compressor is put off in the morning and in the afternoon, so that laborers working inside the cold storage for loading and unloading as well as for re-arranging the potatoes could work for longer duration without feeling excessive cold. On the other hand the compressor is operated for longer duration in the night, to reduce the load on the electrical grid. Thus the huge quantity of potatoes in the chamber itself act as storage of cold and minimizes temperature fluctuations.

2.4 Simulation of potato cold storage

Since the data available in the field survey are in the form of compressor on/off timings, this gives the cooling load a profile in the form of a rectangular wave with high and low of full load and zero load. Though this gives rough idea of total cooling load by averaging the area under the curve, still it does not give the continuous variation of the cooling load with time depending upon outside weather conditions and product stored inside the storage. In order to achieve this goal computer simulation of the GOPI potato cold storage is carried out.

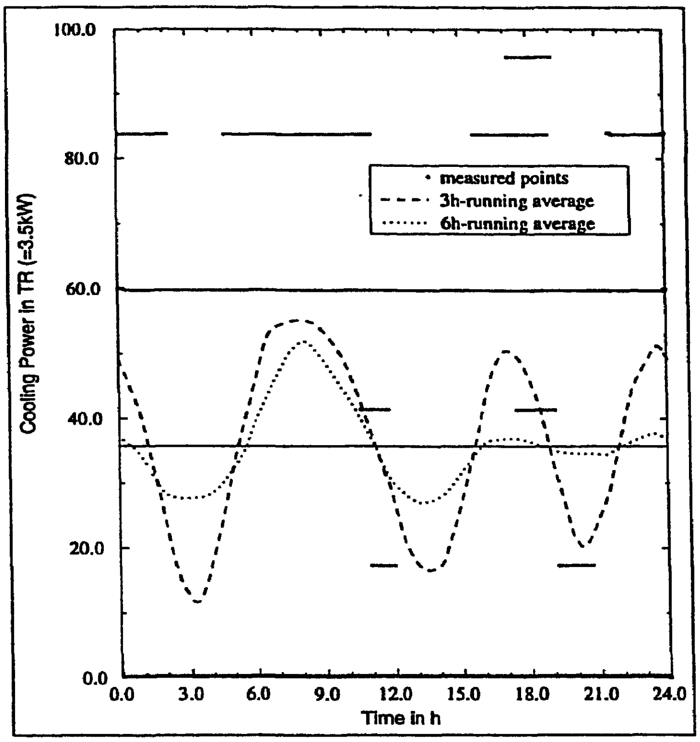


Figure 2.5: Cooling load profile in terms of refrigerant compressor on/off time of GOPI cold storage, Hapur (7200 MT capacity), data of approximately 60 days

Potato storage pattern

It is assumed that the loading operation starts in the middle of February (i.e. 15th onwards) and full capacity is achieved in 45 days time i.e. by March 31st. After that the cold storage gets emptied steadily (linear downward profile) and becomes empty at end of October. The respiration rate of 4064 kJ/t day is taken for potato at 20°C which falls gradually to 1760 kJ per ton per day when desired cold storage temperature of 1.6-3.3°C is achieved in the span of 15 days.

Simulation results

For the purpose of simulation, SUNCODE software [13] for thermal analysis of building is used. The cooling load profile obtained through simulation exercise for GOPI potato cold storage is given in Fig. 2.6.

It can be observed that cooling load increases with loading of potatoes and reaches maximum (175-185 kW_{th} $\simeq$50-53 TR) in the month of April when potatoes storage is at full capacity and outside weather is also getting warmer due to start of hot summer season. Later on the latent heat load due to the respiration of

Capacity:	90000 bags $\simeq$ 7200 MT potatoes (1 bag = 80 kg potatoes)
Location:	extreme east among 4 cold storage chambers
No of floors:	8 floors (of 2.4 m height each) out of which top floor is empty and used for locating evaporator coils
Size:	39 $\times$ 30 $\times$ 16.8 m (partition between floors is 25 $\times$ 25 mm wooden strips with 25 mm gap, in short no rigid partition). 39 m length side is facing east.
Wall:	360 mm thick brick wall (with outside plaster), 390 mm thick rice husk insulation layer from inside, 100 mm thick inner brick wall (i.e. rice husk is filled between 360 mm outer and 100 mm inner brick wall). No plaster inside.
Roof:	Concrete slab (100 mm thick) outside, 230 mm air gap on inner side between concrete slab and 390 mm thick rice husk layer above asbestos cement sheets (2-3 mm thick).

Table 2.2: Hapur cold storage chamber details

ɔtato and also the quantity of potato stored due to its gradual withdrawal re- ıces. This results in lowering the cooling load from its maximum level in April, ʼen though outside weather gets hotter in the peak season on June-July. Cooling ad reduces to minimum (50-60 kW_{th} $\simeq$15-17 TR) in the month of October as orage becomes almost empty by then and outside weather also starts cooling ɔwn as winter season approaches.

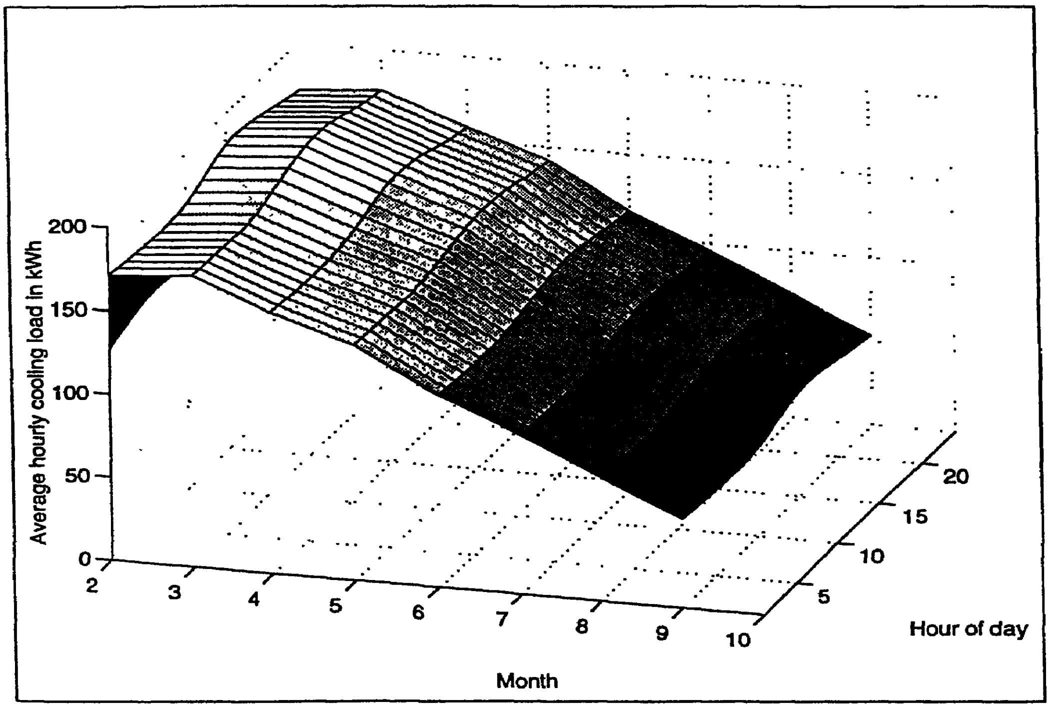


Figure 2.6: Simulated cooling load profile for GOPI potato cold storage

Chapter 3

Adsorption Cooling with Methanol/Silicagel

Parallel to the development of system design for a solar hybrid cooling plant, the adaption of the available cooling process to the special demands is investigated. After the evaluation of the general practicability, an adsorption cooling test plant is set up to prove the theoretical results by experiments.

Due to the use of solar collectors and genset waste heat, the concept requires a refrigeration system which can be driven by heat of a low temperature level. Single stage sorption cooling system are operated with a fixed temperature difference between driving water inlet and outlet of 5-10 K. High inlet temperatures therefore result in high outlet temperatures, which cause bad operation conditions for the solar field and the genset cooling water heat exchanger. By means of an adsorption system, as the cooling system with the working pair water/silicagel, which is available on the market[3], it is possible to reach cold water temperatures of 3°C with driving temperatures of 85°C (COP=0.5, T_c = 29°C). This system can be operated already with driving heat temperature of about 60°C. Thus it would be possible to run the cooling system with flat plate collectors, what might improve the economy because of the lower investment cost.

Due to the used refrigerant water up to now the adsorption chiller is restricted to cooling temperatures above the freezing point of water at 0°C. It will be shown later, that by changing to the working pair methanol/silicagel it might be possible to reach cold brine temperatures of -5°C with an COP=0.25.

Another option might be a new development in the field of ammonia-water absorption heat pumps. By parallel research, there is now a new technology available at DLR, which improves the performance of a common single stage absorption system as much, that these might be suitable for the cooling using low temperature heat source ($<$ 100°C).

To get predictions for the use of methanol instead if water for the adsorption chiller, the process is first analyzed for operation with water, which can be compared with the data of the commercial system. After an introduction to the thermodynamics a theoretical analysis is carried out for a prediction of the COP for methanol/silicagel. By experiments with a test facility this is validated.

3.1 Thermodynamics

3.1.1 Principle of operation

The principle of an adsorption cooling system is depicted in Fig. 3.1. Similar to a vapor compression system it is built up with a condenser, a throttle a valve, an evaporator and a compressor. However in this system the compressor is operated by a thermal sorption process instead of a mechanical compressor.

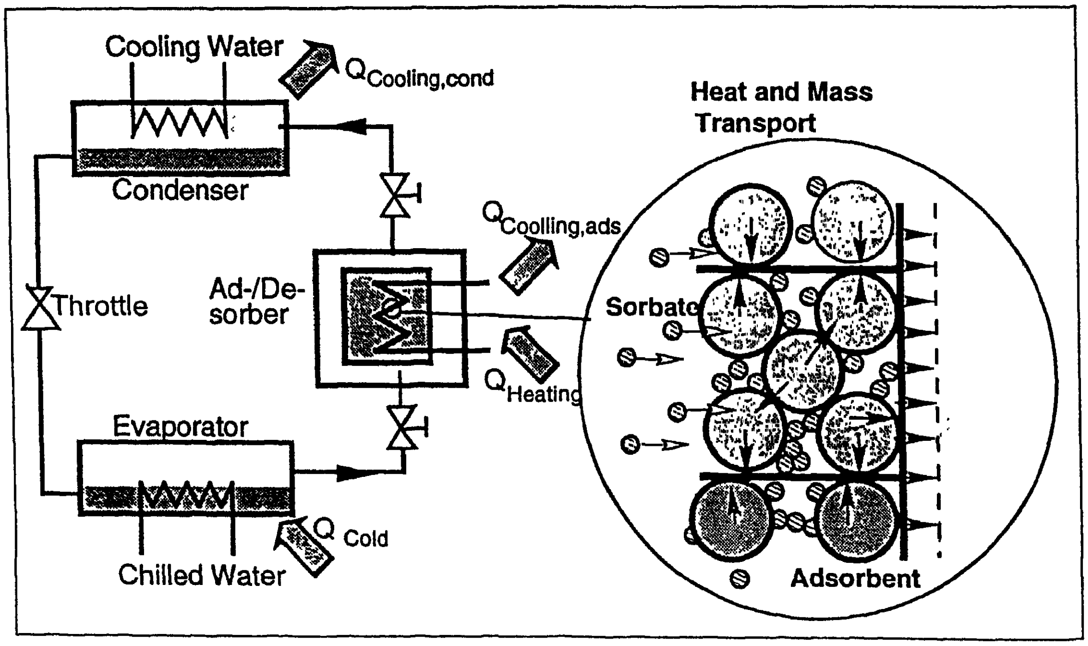


Figure 3.1: Working principle of adsorption cooling system

The thermal compressor is operated in two phases. During the first phase of the operation cycle the refrigerant is evaporated at low pressure and low temperature in the evaporator and is adsorbed by the silicagel in the reaction chamber under isobaric conditions. In the second phase the loaded adsorbent is regenerated by heating up the adsorbent (temperature swing) or lowering the pressure (pressure swing).

In the reaction chamber (ad- and desorber) the refrigerant is adsorbed in the pores of the adsorbent silicagel by physical and chemical effects. The heat of adsorption, which is set free in this mass transfer process is removed by a heat exchanger in the reaction chamber with the cooling water. The lower the cooling water temperature the higher the final uptake of refrigerant by the silicagel will be.

After saturation of the silicagel the mode of operation is changed and the adsorbent is regenerated by an isosteric heating up of the adsorbent and a following isobaric desorption. The pressure for this second part of the cycle is given by the point of saturation in the condenser, which is fixed by the cooling water temperature.

Before the next adsorption, the sorbens is cooled down isosteric and the condensed refrigerant is fed by an expansion valve to the evaporator. By this two step ad- and desorption process the refrigerant is compressed.

The steady state loading C of the adsorption, defined as the uptake of adsorbate by the adsorbent,

$$C = \frac{m_{\text{adsorbate}}}{m_{dryadsorbent}} \tag{3.1}$$

is a function of pressure p and temperature T

$$C = C(p, T). \tag{3.2}$$

The relation between pressure and temperature in the steady state is described by the equation of Clausius-Clapeyron

$$\frac{\mathrm{d}p}{\mathrm{d}T} = \frac{\Delta h_d}{T \Delta v}, \tag{3.3}$$

with the heat of adsorption Δh_d and the phase change volume Δv.

If the volume of the fluid v_f is negligible compared to the volume of the gaseous phase v_G, the phase change volume Δv can be set to the volume of the gaseous phase, for which the ideal gas theory can be applied

$$\Delta v = v_d = \frac{RT}{p}. \tag{3.4}$$

The result after integration with equation (3.3) is

$$\ln p = -\frac{\Delta h_d}{R} \frac{1}{T} + const.. \tag{3.5}$$

Thus the lines on constant uptake can be plotted as lines in a log(p)-1/T-diagram, which is called Clapeyron diagram. In Fig. 3.2 the process of adsorption cooling is plotted in the Clapeyron diagram.

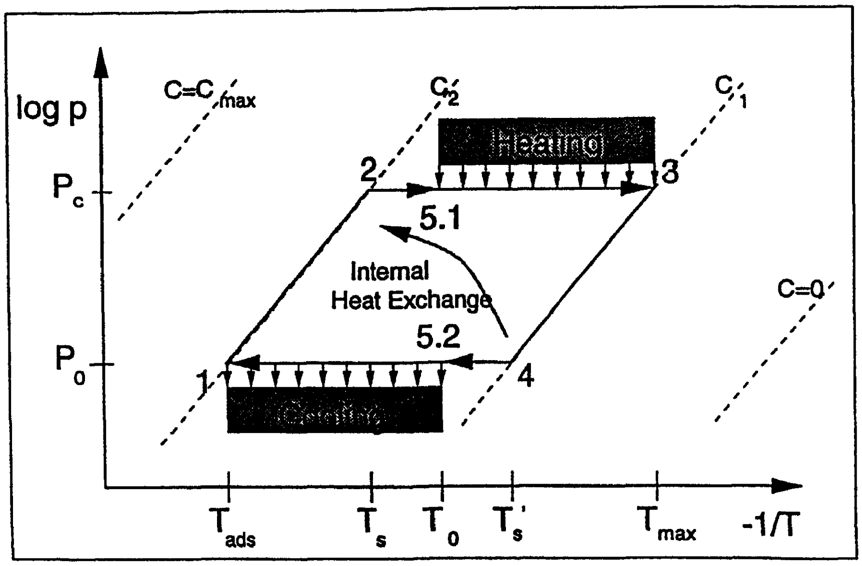


Figure 3.2: Clapeyron diagram of adsorption cooling system

The ideal process is displayed as a rhombus in the Clapeyron diagram between the isosteres C_2 and C_1 ($C_1 < C_2 < C_{max}$) and the isobares p_c and p_0.

To reach an equable power output, the system can be modified as two chamber system, which is operated in a cycle (Fig. 3.3). By an internal heat exchange between the two chambers during the isosteric heating and cooling of the sorbens, the efficiency of the system can be improved.

3.1.2 Transient behavior

The uptake of the sorbens C depends on the time. A typical profile for the uptake is given in Fig. 3.4. Starting from the initial uptake C_0 for very long times the final uptake C_{max} will be reached, which is defined by the cooling water temperature T_c and the evaporator pressure p_0.

For isothermal adsorption this is described according to Sakoda[12] by

$$\frac{dC(t)}{dt} = k_s a_p (C_{max} - C_0), \tag{3.6}$$

with the temperature depending mass transfer coefficient $k_s a_p(T)$

$$k_s a_p = \frac{c_1}{r^2_{particle}} \exp(-\frac{c_2}{T}). \tag{3.7}$$

The cooling power $\dot{Q}_c$ is determined by the amount of adsorbed refrigerant. Due to the steady state in evaporator and adsorber, only as much refrigerant can be

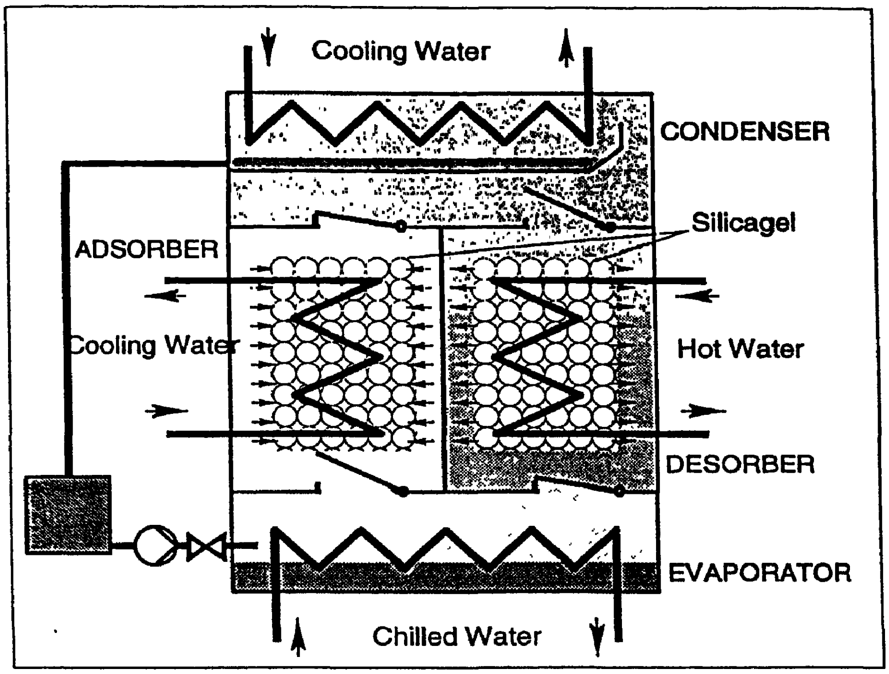


Figure 3.3: Two chamber adsorption cooling system

evaporated as is adsorbed. Otherwise the pressure p_0 raise and causes a higher evaporation temperature. Thus the actual cooling power is given by

$$\dot{Q}_c = \frac{\mathrm{d}C(t)}{\mathrm{d}t} m_{dryadsorbent} \Delta h_{ads}. \tag{3.8}$$

3.1.3 Influence of operation parameters on the coefficient of performance

For heat pumps it is difficult to use the typical efficiency ($0 < \eta = \frac{\text{Output}}{\text{Input}} < 1$). By the ratio of evaporation energy Q_0 to desorption energy Q_{des} however a coefficient of performance COP can be defined

$$COP = \frac{Q_0}{Q_{des}}, \tag{3.9}$$

which describes the cooling system.

Theoretically values for the COP up to 2-3 are possible. In fact however feasible systems have always lower values due to thermal losses.

A thermo-dynamical analysis of the adsorption chiller with methanol, operating at -2°C, gives the limits for the technical possible COP.

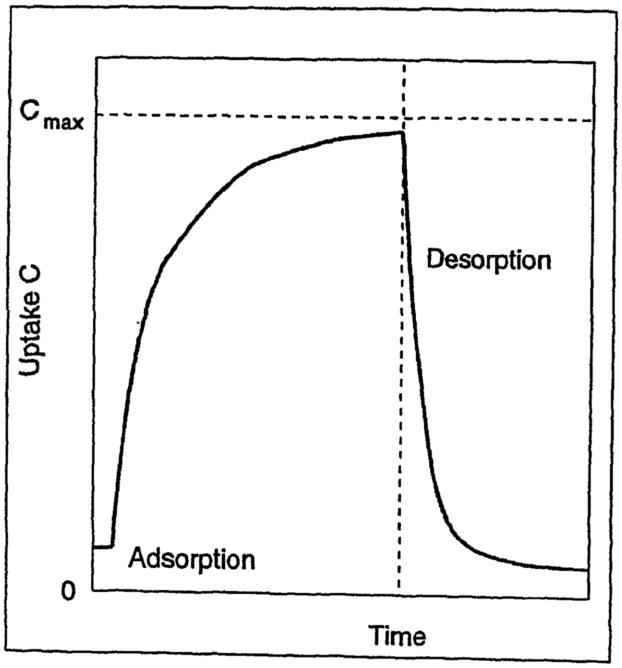


Figure 3.4: Time dependent uptake

Refrigerant	Δh_V at $p = 0,1$ bar in J/g	Δh_D at $C = 8\%$ in J/g
Water	2400	3020
Methanol	1200	1680

Table 3.1: Heat of vaporization and adsorption by silicagel [7]

The COP for a cooling system is generally limited by the efficiency given by the reversible Carnot cycle

$$COP = \frac{Q_0}{Q_h} = \frac{T_0(T_h - T_c)}{(T_c - T_0)T_h}, \tag{3.10}$$

with the temperature of the heating source T_h, the brine/cold water temperature T_0 and the cooling water temperature T_c.

The achievable COP depends according to equation (3.10) on the operating temperatures. For lower brine temperatures the maximal COP decreases due to thermodynamics.

By the lower ratio of phase change energy Q_{desorb}, which is a material property of the refrigerant (Tab.3.1), to energy needed for heating up Q_{heatup}, which mainly is influenced by the system design, the working pair methanol/silicagel has a lower

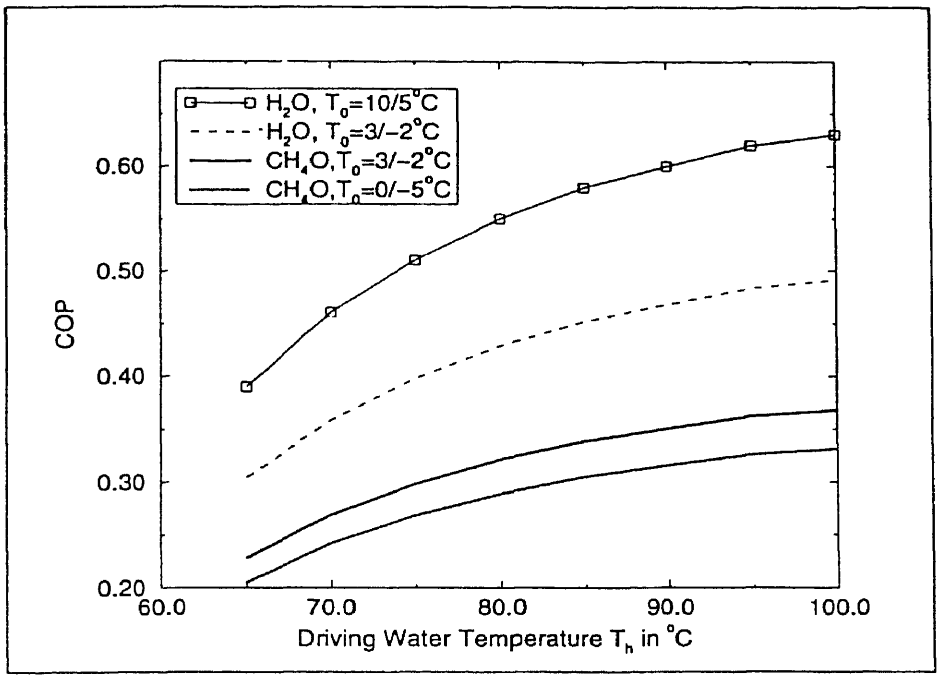


Figure 3.5: Predicted COP for methanol (CH_3OH) (Curve for water at 3/-2°C is based on theoretical calculations)

COP compared to water/silicagel

$$COP_{period} = COP_{cont}\frac{1}{1 + Q_{heatup}/Q_{desorb}}. \tag{3.11}$$

Taking also the losses of the cooling system into account, it is possible to predict the COP for the methanol/silicagel cooling system (Fig. 3.5). Lowering of the brine temperature results in an COP for brine temperature $T_{chilled} = 3/-2$°C, which is about 75% of the COP for $T_{chilled} = 10/5$°C.

The lower ratio of phase change energy to energy needed for heating up reduces the COP for methanol/silicagel additionally of about 25% compared to the system water/silicagel

$$COP_{CH_3OH} \approx 0.75\, COP_{H_2O}.$$

Thus the predicted COP for methanol at the brine temperature $T_{chilled} = -2$°C is about half of the COP for water at cold water temperature $T_{chilled} = 5$°C. Based on the data of a commercial water/silicagel chiller the COP for the methanol/silicagel system will range between 25-32%, depending on the driving water temperature.

3.2 Laboratory test facility for adsorption

A laboratory test facility has been built up at DLR (Fig. 3.6 and 3.7), to examine the actual operational conditions for an adsorption cooling system with the working pair methanol/silicagel.

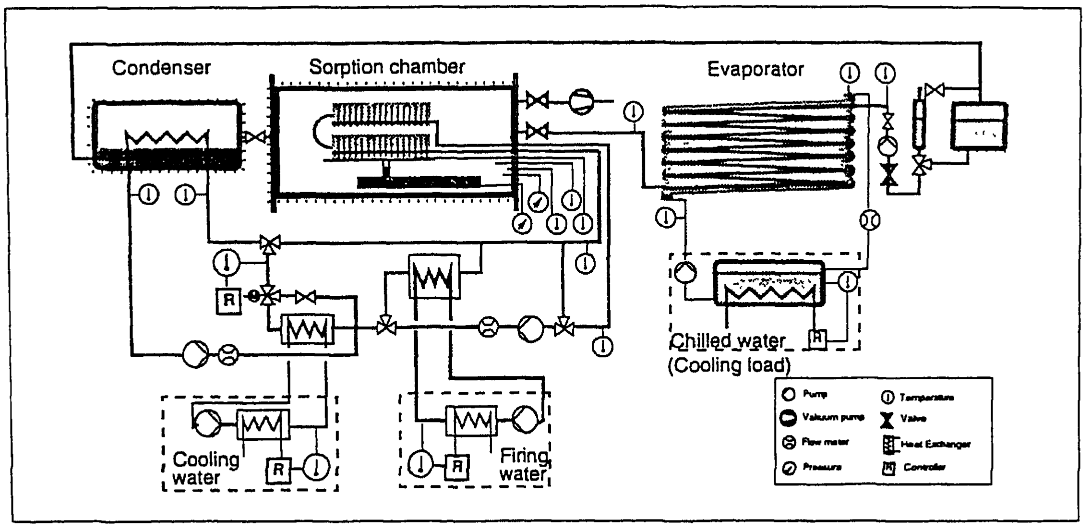


Figure 3.6: Scheme of the adsorption test facility at DLR

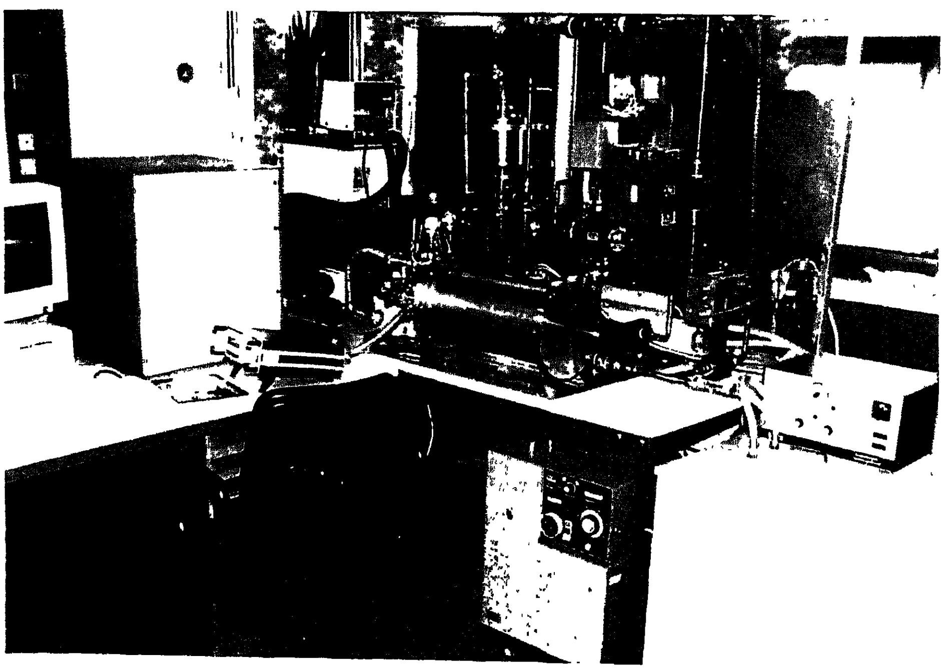


Figure 3.7: Adsorption test facility at DLR

Sorption chamber	Volume Mass of silicagel	23.9 l 0.6 kg
Cooling water	Temperature range Power at (20 °C)	0-40 °C 2 kW
Firing water	Temperature range Power	20-95 °C 6 kW
Evaporator	Temperature range Power (at 0 °C)	-5 - +30 °C 2 kW

Table 3.2: Data of the adsorption test facility

The maximum power of the components of the test facility is about 2 kW, depending on the working pair and the operating temperatures. (Tab. 3.2).

The central part of the system is the vacuum chamber. In the chamber a finned tube heat exchanger packed with silicagel is placed on an electronic scale to record the weight of the sorbens. By this the uptake of the silicagel with refrigerant can be evaluated. Additionally also pressure and temperature in the reaction chamber are recorded.

For all heating and cooling loops mass flows as inlet and outlet temperatures for the heat exchanger are available, to calculate heat transfers in the components.

3.3 Experiments

As the test facility differs in their results due to the down scaling, the design and the used materials, experiments are carried out with water and methanol as refrigerant. Thus the effect of the different physical properties (e.g. the boiling temperature, Fig. 3.8) can be studied. Comparing the results predictions for a modified chiller can be done by up-scaling.

3.3.1 Refrigerant Water

Several cycles of ad- and desorption are carried out at operation conditions of heating water with $T_h = 85°C$, cooling water $T_c = 30°C$ and an evaporator temperature, which corresponds to the chilled water temperature of $T_0 = 5°C$. Between ad- and desorption phase the sorption chamber heat exchanger is operated for some minutes in bypass mode. By this the heating/cooling loop is tempered for the new operation temperature. This also corresponds to the internal heat exchange phase of the two-chamber system.

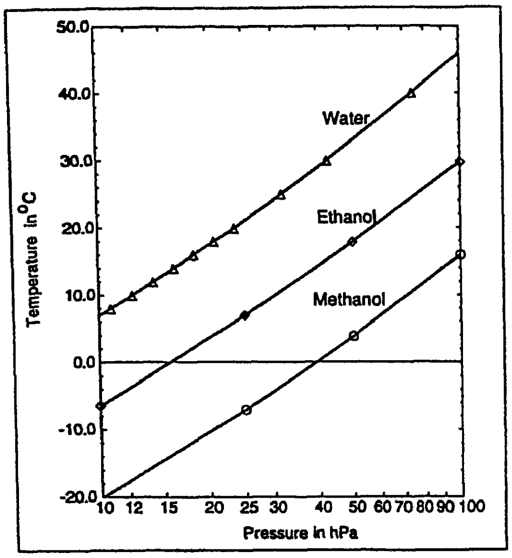


Figure 3.8: Boiling point curve for different refrigerants

Uptake

The process is displayed very significantly by the time profile for the uptake C. In Fig. 3.10 four cycles are displayed. Each of the adsorption phases takes about 50 min, whereas the desorption is completed in about 15 min. The difference in the mass transfer is mainly caused by the temperature dependence of the mass transfer coefficient. Together with the bypass operation a complete cycle takes about 70 min.

The uptake of the silicagel oscillates under the given conditions between 6 and 11%. This corresponds quite well with the data from isosteric charts of Khelifa for the silicagel 'Trockenperlen N'[7], which is displayed in Fig. 3.9. Deviations in the maximum and minimum values are caused by variation in the heating or cooling temperatures.

During the adsorption the pressure in the chamber is regulated by the evaporation pressure of water in the evaporator $p_0(T_0 = 5°C) = 10$ hPa. For a cooling water temperature $T_c = 30°C$ the resulting maximum uptake C_{max} is 15%. If this temperature is not reached in the sorbens the maximum uptake will be reduced (e.g. $C_{max} = 11\%$ for $T_c = 35°C$). The maximum value is reached for very long times, whereas at technical applications the process is stopped earlier, to improve the power density. The minimum uptake is limited by the heat source temperature $T_h = 85°C$. With the condenser pressure $p_c(T_c = 30°C) = 40$ hPa the ideal limit is close to 4%. Due to the limitations of the technical process and the temperature gradient in the silicagel only an oscillation between 6 and 11% is reached in the experiment for $T_c = 30°C$, $T_0 = 5°C$ and $T_h = 85°C$.

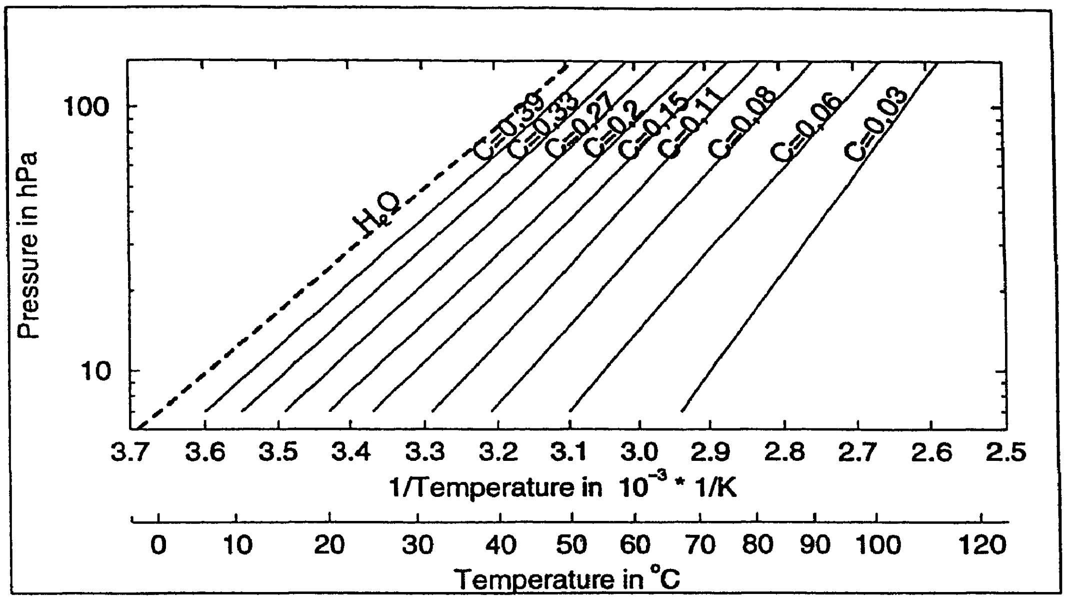


Figure 3.9: Isosteres for water/silicagel (Trockenperlen N) [7]

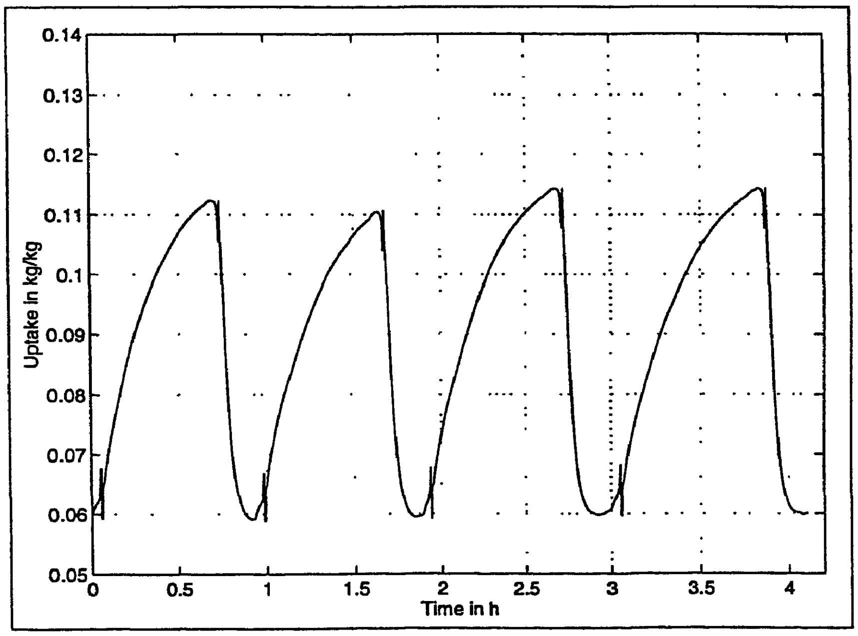


Figure 3.10: Uptake for water/silicagel $T_0 = 5°C$, $T_h = 85°C$ $T_c = 30°C$

Process in the Clapeyron diagram

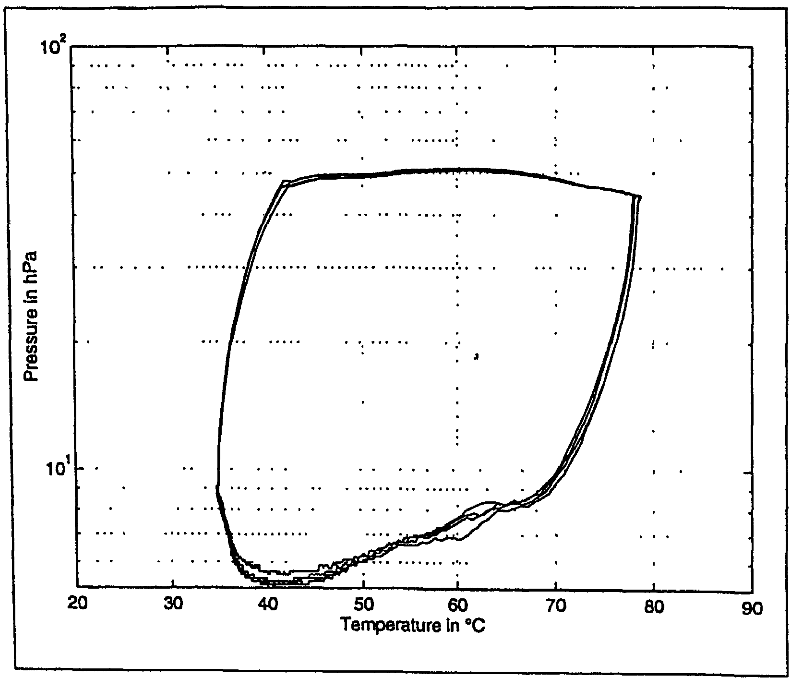


Figure 3.11: Measured temperature-pressure curve in the Clapeyron diagram for water/silicagel

Plotting the pressure in the sorption chamber over the temperature of the sorption chamber (Fig. 3.11), the result confirms the ideal cycle displayed in Fig. 3.2. The pressure level for isobaric ad- and desorption is fixed by evaporator and condenser temperature, whereas the isosteric heating and cooling is fixed by the temperature in the heat exchanger of the sorption chamber.

3.3.2 Refrigerant Methanol

Operating the system with the same border condition as for water, the resulting loading is nearly the same when using methanol as refrigerant (Fig. 3.12). The uptake during adsorption at an evaporator temperature of $T_0 = 5°C$ ($p_0 = 28$ hPa) and a cooling temperature of $T_c = 30°C$ is nearly 13.5%. The regeneration of the adsorbent reaches 8.5% at an heating water temperature of $T_h = 85°C$ and a condenser temperature $T_c = 30°C$.

Operating at the same temperature levels, as a water/silicagel, the pressure at normal boiling is higher due to the lower evaporation temperature for methanol. Thus the resulting uptake is as much as with water, compensating a worse adsorption process.

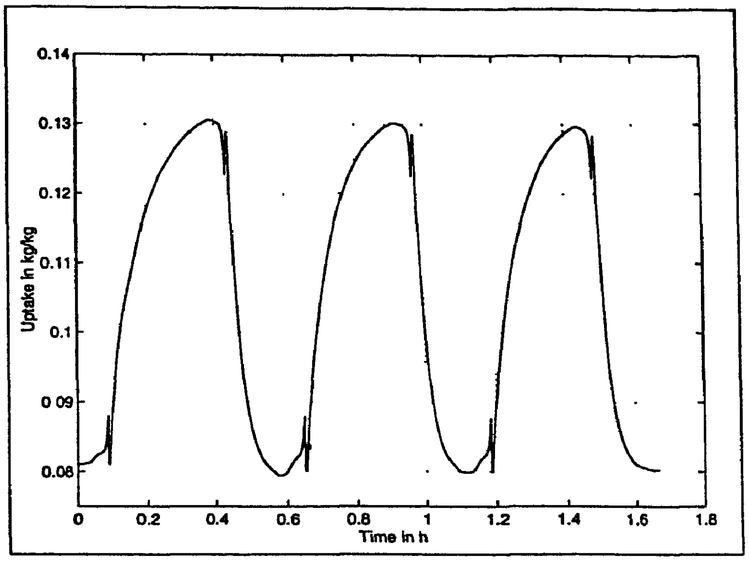


Figure 3.12: Measured uptake for methanol/silicagel $T_0 = 5°C$, $T_h = 85°C$ $T_c = 30°C$

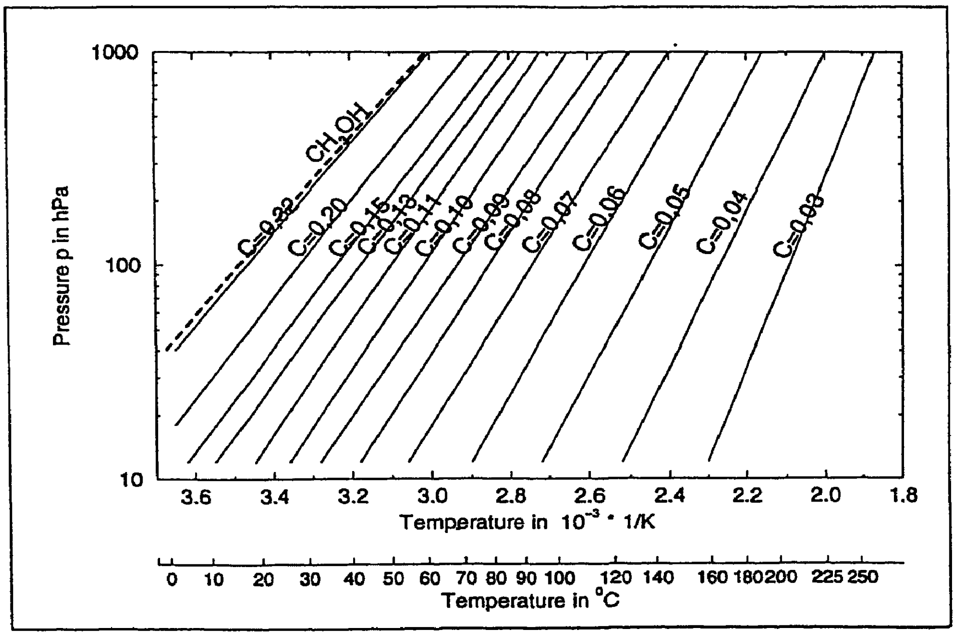


Figure 3.13: Isosteres for methanol/silicagel (Trockenperlen N) [7]

3.3.3 Comparison of water and methanol as refrigerant

The uptake profile of a refrigerant/adsorbent -pair describes well the heat and mass transfer behavior. More relevant for the technical application however is the power output of the chiller.

Cooling power

In Fig. 3.14 and 3.15 curves for the transferred heating and cooling power using water or methanol are displayed. These charts correspond to the ideal curve, resulting from product of uptake and specific heat of adsorption (equation 3.8). The small peaks e.g. at t=0.1 h and t=0.45 h are caused by the bypass operation, due to restrictions of the test facility. The peaks for negative power are caused by the regeneration phase, when energy is needed for desorption.

Whereas the amount of absorbed mass is nearly the same for both refrigerant, the resulting integral cooling power for the two refrigerants is different. This is

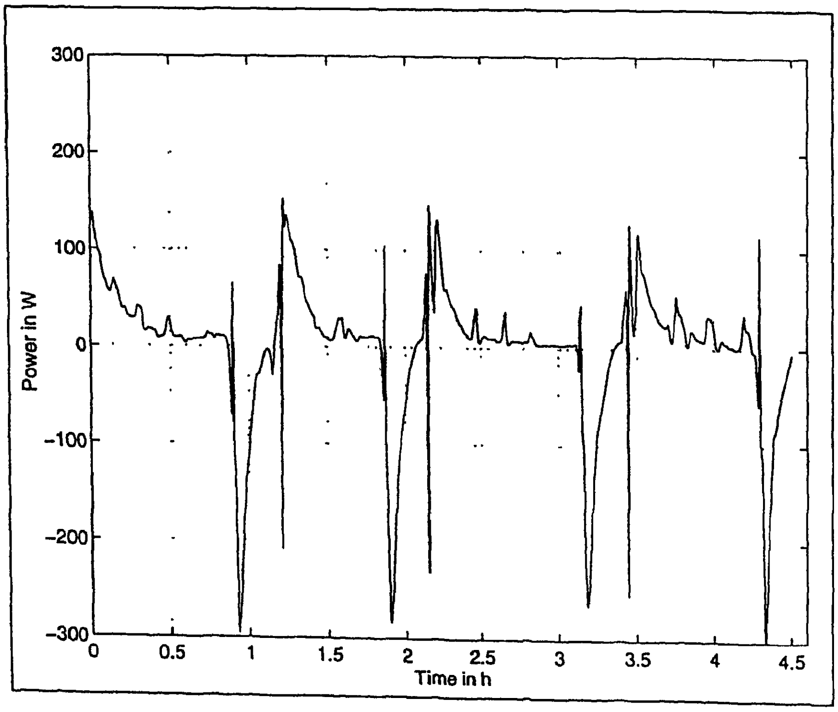


Figure 3.14: Measured cooling power for water/silicagel at $T_0 = 5°C$, $T_h = 85°C$ $T_c = 30°C$

caused by the different heat of vaporization and adsorption (Tab. 3.1). Methanol has about half of the latent heat for the phase change of water and thus the

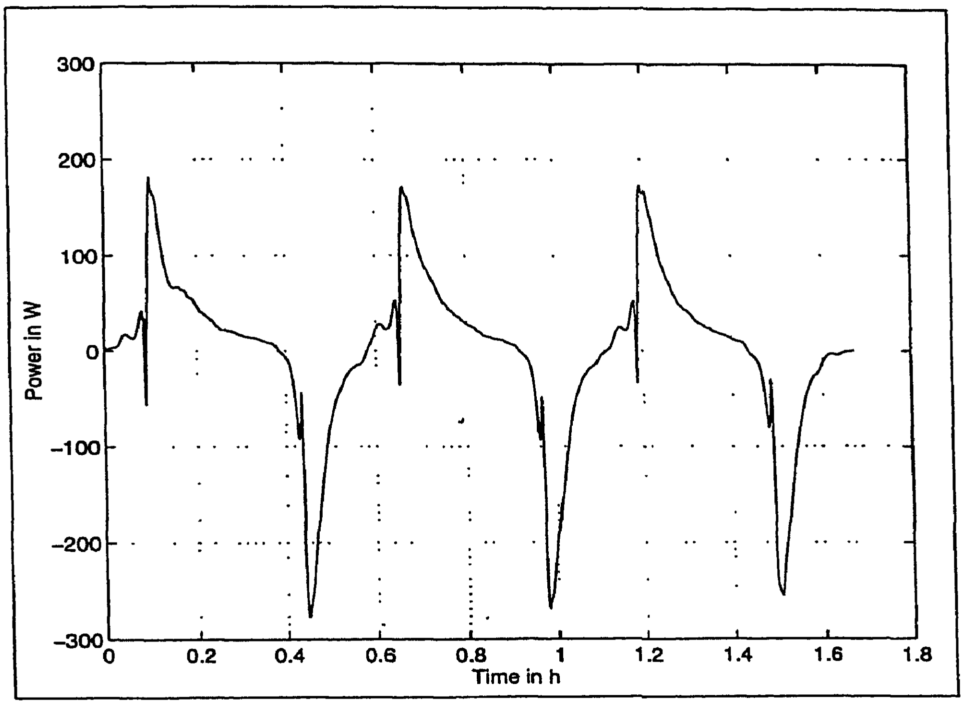


Figure 3.15: Measured cooling power for methanol/silicagel at $T_0 = 5°C$, $T_h = 85°C$ $T_c = 30°C$

resulting turnover of energy is less. The integral energy absorbed during one cycle is higher for water, the adsorption process however takes nearly double the time(0.8 h for water, 0.3 h for methanol).

As the energy required to heat up and cool down the heat exchanger and the silicagel between ad- and desorption is the same for both refrigerants. The lower amount of energy used for the phase change results in a lower COP.

Operation below 0°C

According to the boiling point curve the evaporation pressure is reduced and so is the maximal uptake of the adsorbent. When lowering the boiling temperature to -2°C the evaporation pressure is about $P_0 = 20$ hPa and the maximal uptake is about 11.3% (Fig. 3.16). The evaporation temperature effects only the maximal uptake, whereas the minimal uptake at regeneration is not influenced by the evaporation temperature. If possible, the regeneration temperature should be raised, to enlarge the amount of adsorbed refrigerant and thus to improve the performance data.

Without rising the firing water temperature the resulting chiller power is reduced

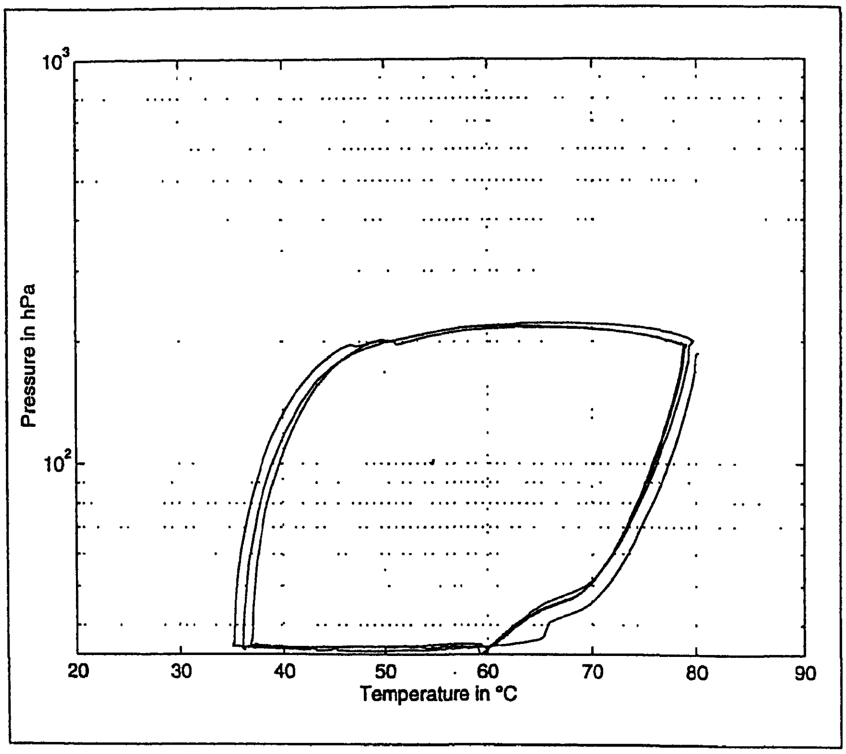


Figure 3.16: Measured temperature-pressure curve for methanol/silicagel at $T_0 = -2°C$, $T_h = 85°C$, $T_c = 30°C$ in the Clapeyron diagram

to an average value of about 10 W/kg (Fig. 3.17, Tab. 3.3).

3.3.4 Adsorption data of commercial system

For a prediction of the use of methanol/silicagel in a commercial application the results for water/silicagel of the test facility with the data of the commercial system can be compared. Extrapolating this relation of water informations for the methanol/silicagel can be achieved.

Comparing the specific power of a commercial systems with the results of the test facility shows that the power density is only about 1/15 (Tab. 3.3). The much higher power density of the commercial system is mainly reached by a silicagel with a better sorption kinetic, which is not available in Europe. By this adsorption and regeneration cycle takes less time and thus the resulting chiller power is higher. It can be assumed, that similar to water also with methanol as refrigerant a higher power density (100 W/kg) can be achieved.

In Fig. 3.18 the temperature profiles for such a system are given. The operation period for this two-chamber system is about 6 min.

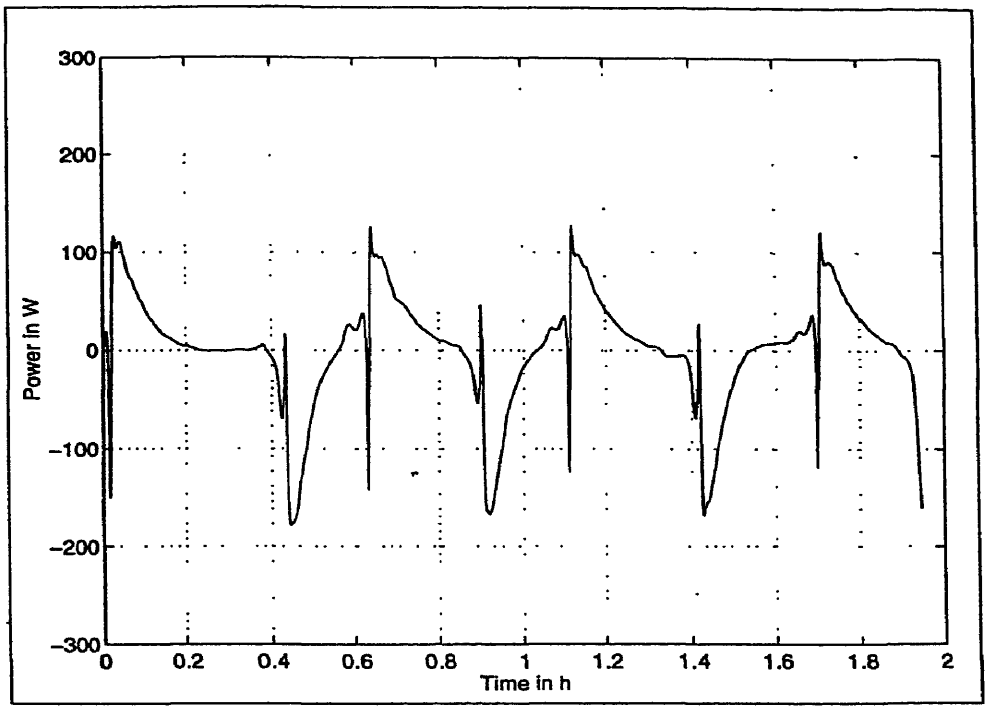


Figure 3.17: Measured cooling power for methanol/silicagel at $T_0 = -2°C$, $T_h = 85°C$, $T_c = 30°C$

The COP for the commercial system at the selected point of operation ($T_0 = 5°C$, $T_h = 85°C$, $T_c = 30°C$) is about 0.58.

	Test facility			Commercial System
Refrigerant	Water	Methanol		Water
Evaporator Temperature	5C	5C	-2C	5C
Transfered Energy	70 kJ	35 kJ	25 kJ	360 kJ
Cycle period	60 min	60min	60min	6 min
Mass of silicagel	0.6 kg	0.6 kg	0.6 kg	200 kg
Specific power	30 W/kg	15 W/kg	10 W/kg	300 W/kg

Table 3.3: Specific power density

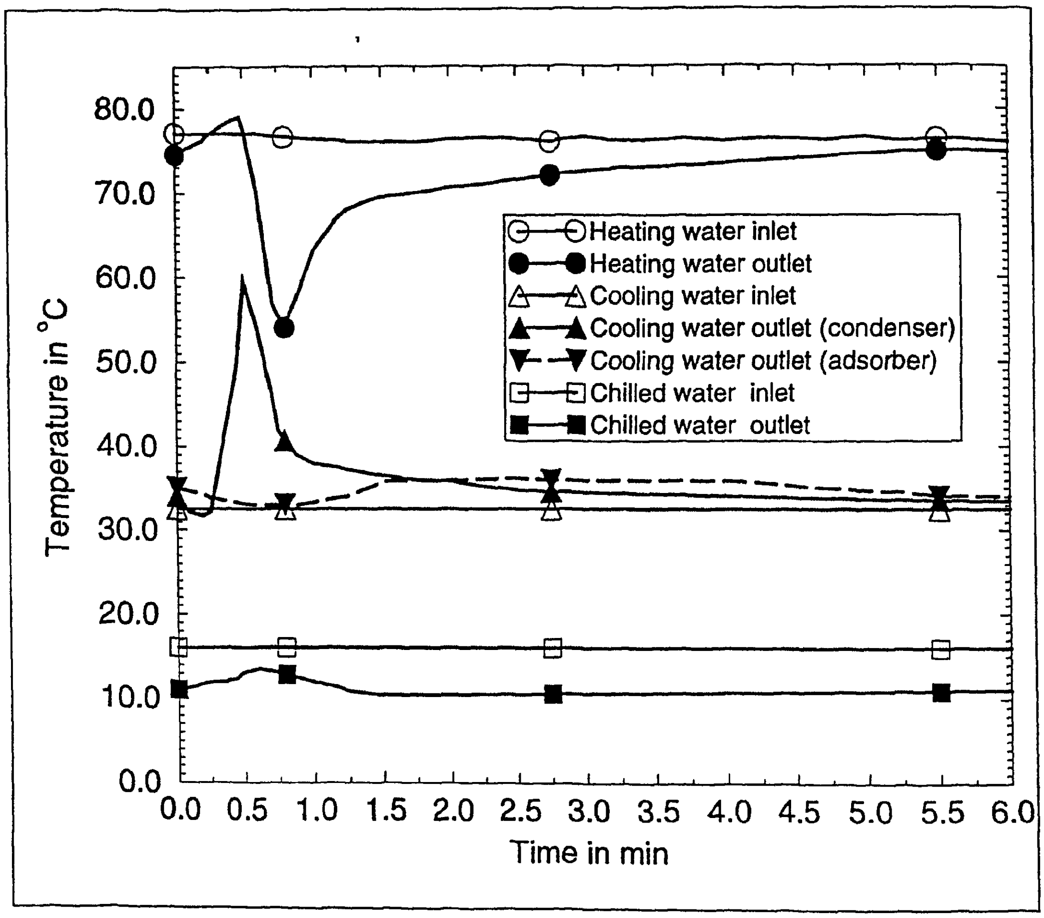


Figure 3.18: Temperature profiles of commercial adsorption chiller [3]

Chapter 4

System Design

The system design is done in several steps. First a preliminary conception of the system is made to check technical feasibility and economics. With the results of the preliminary conception a second (modified) system is developed without using a boiler, but an larger genset. For this system again an economic analysis is carried out. Additionally a CO_2-analysis is prepared. After proving the feasibility the component parameters are optimized by a parametric study.

4.1 Preliminary conception of test plant

4.1.1 Description of the preliminary system

By calculations it has figured out, that a stand-alone solar application would require a very large storage for continuous operation. This causes high thermal losses and would also effect high costs.

It seems to be more convenient, to combine the solar system with a backup system. The combination with biomass is promising, because on one side there is only a limited amount of biomass available and on the other side the solar part can be designed to cover the main load during the day.

In Fig. 4.1 the preliminary system concept is depicted. The basic components are the collector field, the buffer tank, the auxiliary heater and the refrigeration system with the cooled room. The bypass control for the collector loop enables to run the collector field on a fixed outlet temperature.

A generator, fired by diesel and producer gas is intended for producing electricity to operate the plant as a stand-alone-system. The producer gas is provided by a gasifier and is used for the boiler as well.

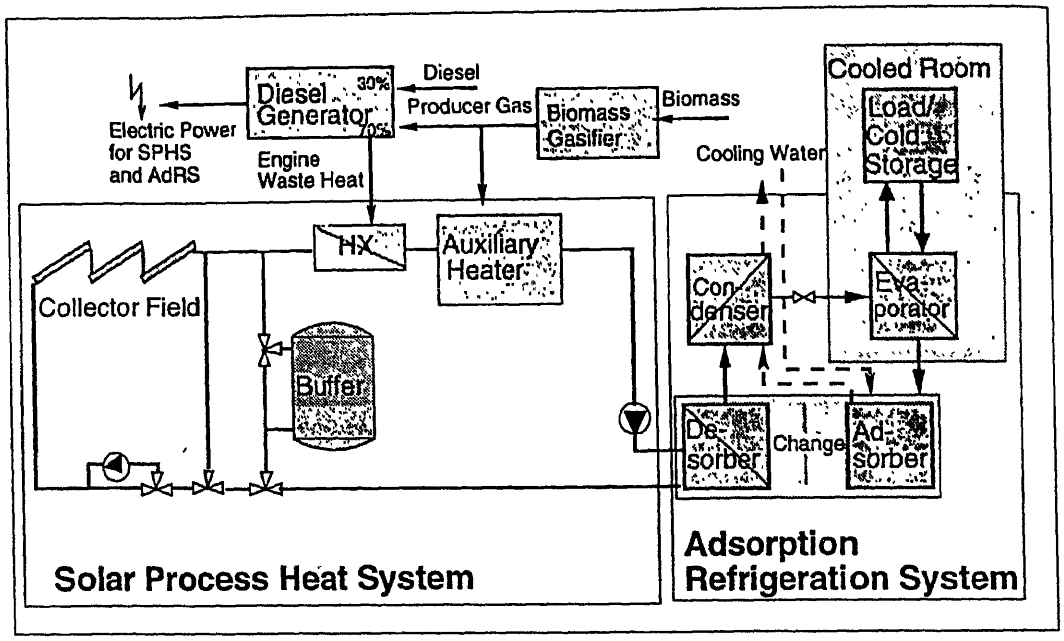


Figure 4.1: Preliminary system concept

The waste heat of the genset will be used, to heat up the firing water of the sorption refrigeration system.

4.1.2 Economic analysis

System configuration The heat input required for operation of the vapor adsorption refrigeration system (VAdRS) is provided by combination of following heat sources,

- hot water input from the solar flat plate collectors (FPC) located at the roof, whenever solar insulation is available.
- waste heat from the genset exhaust gases is recovered to the extend possible through heat exchangers, and
- balance heat requirement is met by burning the producer gas obtained through gasification of biomass in the gasifier and utilizing this heat for heating the sufficient quantity of water to desired temperature required for operation of VAdRS.

The assumptions, which had been made in carrying out the economic analysis are shown in Tab. 4.1.

System parameters	
Cold storage capacity	2000 MT
Solar panel area	100 m^2
Solar collector efficiency	25%
VAdRS capacity	182 kW_{th}
COP of VAdRS	0.4
VCR capacity	140 kW_{th}
Boiler efficiency	80%
Cost parameters	
Biomass/wood cost	0.4 Rs/kg
Diesel cost	7.0 Rs/kg
Electricity purchase price	3.0 Rs/kWh
Solar collector cost	6.000 Rs/m^2
Gasifier cost	350 Rs/kW heat rate
VAdRS cost	25,000 Rs/kW_{th} (nominal power)
Conventional system cost	4,000 Rs/kW_{th} (nominal power)
Pay-back period calculation	
Investment in conventional	364,000 Rs
Investment in VAdRS	5,442,683 Rs
Incremental investment cost in VAdRS	5,078,683 RS
Simple pay-back period	33.8 yrs
Annual solar fraction	4%

Table 4.1: Parameters for economic analysis (47 Rs $\approx$ 1 ECU)

For more and more solar collector area installed the solar fraction increases and becomes 22% for 500 m^2 collector area but the pay-back period increases to 42 years due to the additional investment of solar collectors.

Considering the fact that the cost of the system goes down as more and more systems are installed and as the technology and scale of production improves. Therefore analysis was carried out for capital investment reduction up to 50% when technology gets commercialized. At this investment levels the pay-back period for increase in price levels (uniform increase in prices of wood, diesel, electricity, etc. is assumed) up to 50% is calculated to see its effect on pay-back period. It can be seen that for system having 100 m^2 solar collector area, pay-back period comes down from 34 years to 15 years with 50% reduction in investment cost and it further reduces to 10 years with 50% increase in price level. The results are summarized in Tab. 4.2.

Capital cost reduction in %	Increase in price level in %	Pay back period for different collector areas in yrs		
		100 m²	300 m²	500 m²
0	0	33.8	38.3	42.1
10	0	30.2	34.3	37.7
20	0	26.6	30.2	33.3
30	0	22.9	26.1	28.9
40	0	19.3	22.1	24.4
50	0	15.7	18.0	20.0
50	10	14.3	16.4	18.2
50	20	13.1	15.0	16.7
50	30	12.1	13.9	15.4
50	40	11.2	12.9	14.3
50	50	10.5	12.0	13.3
Solar fraction in %		4.38	13.15	21.91

Table 4.2: Pay back periods of preliminary system design for reduction in capital cost and escalation in price levels

4.1.3 Simulation

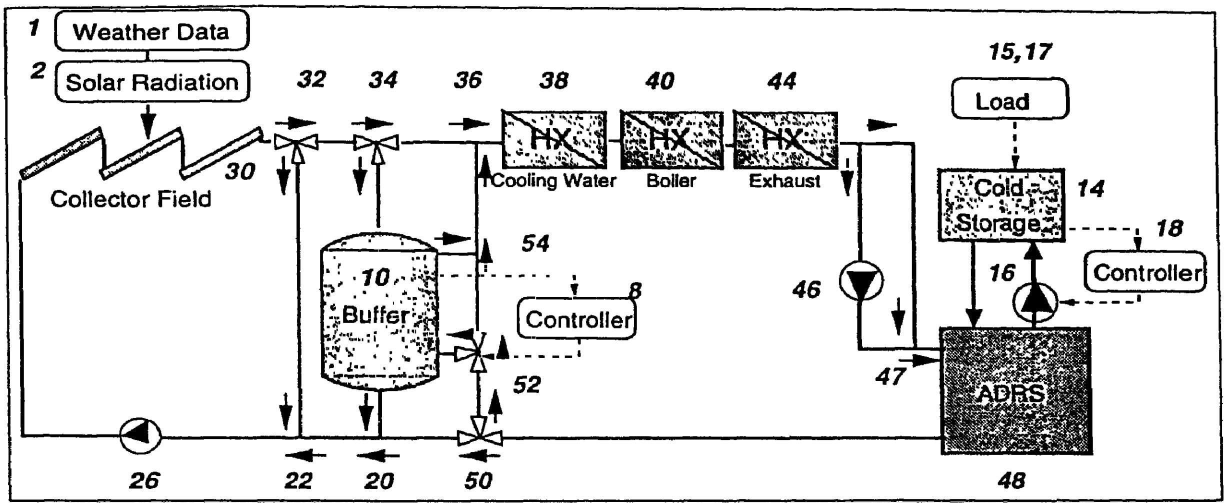
For the simulations the program package TRNSYS[6] is used. TRNSYS is a modular simulation package with physical component models for the simulation of transient solar systems. Every system component is modeled by a subroutine (UNIT), which describes its physical behavior. In an input-file (called deck-file) the characteristic parameters are given for every component and the connections and interaction of all the units are defined by their (INPUTS) and (OUTPUTS).

Due to the modular concept and the available FORTRAN-source code it is no problem to extend it by additional component models. With the extensions, described in section A a simulation model is developed according to the system concept by describing the system in a deck-file.

Additionally to the hardware components (collector, tank, pumps, chiller, heat exchanger, pipes, T-pieces and valves), depicted in Fig. 4.2 and Fig. 4.7 the simulation decks contain control, input and output components.

4.1.4 Preliminary design

In the first approach (Fig. 4.2) the firing water, coming from the collector field or the buffer tank, is heated by the genset cooling water, an auxiliary boiler and the genset exhaust. This enables an easy power backup for insufficient solar input. Simulation shows, that the system operates satisfyingly.



Unit	Component	Unit	Component
1,2,15,17	Data Input	20,22, 36, 47, 54	T-Piece
8,18	Controller	30	Collector
10, 14	Storage tank	32, 34 ,45, 50, 52	Flow diverter
16,26,46	Pump	38, 40, 44	Heat exchanger
48	Adsorption cooling system		

Figure 4.2: Scheme of the preliminary system

The results for 3 days in April are displayed in Fig. 4.3 for a system with the parameters, given in Tab. 4.3. During the first day nearly all of the heat required to operate the adsorption refrigeration system Q_{AdRS} can be supplied by the collector field and the waste heat of the genset. Only in the morning the auxiliary heater has shortly to operate. During the second and the third day there is a higher cooling demand, so that the chiller has also has to be operated during night. By means of the buffer storage it is possible to cover the main part of the heat demand. Again, only in the morning it is necessary to use the auxiliary heater.

The cost analysis however points to the problem of this preliminary system design. The pay back time is very long due to the high investments and the additional operating costs by the use of biomass.

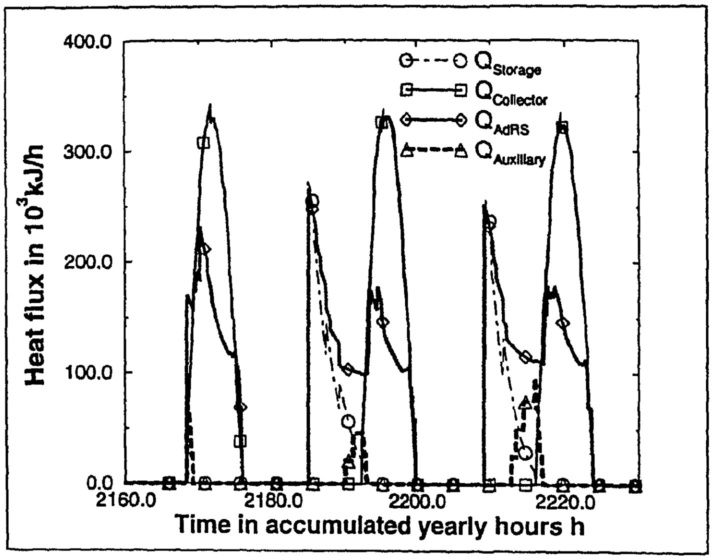


Figure 4.3: Heat fluxes in relevant system components for 4 days in April of the preliminary system

Collector (flat plate)	Outlet temperature	75 °C
	Power (average)	4 kW_{th}
	Power (peak)	16 kW_{th}
	Area	25 m^2
Buffer tank (volume)		5 m^3
Producer gas boiler (power)		15 kW_{th}
Cold storage	Volume	240 m^3 (60t)
	Temperature	3/-2 °C
	Average cooling load	3.5 kW
Adsorption cooling machine	Nominal capacity	10 KW_{th}
	COP	35%
Genset	Power (electric)	1 kW_{el}
	Amount of waste heat (η_{hX}=80%)	1.5 kW_{th}
Solar fraction		20%

Table 4.3: Design parameters of the preliminary solar-hybrid adsorption cooling system

4.2 Modified System

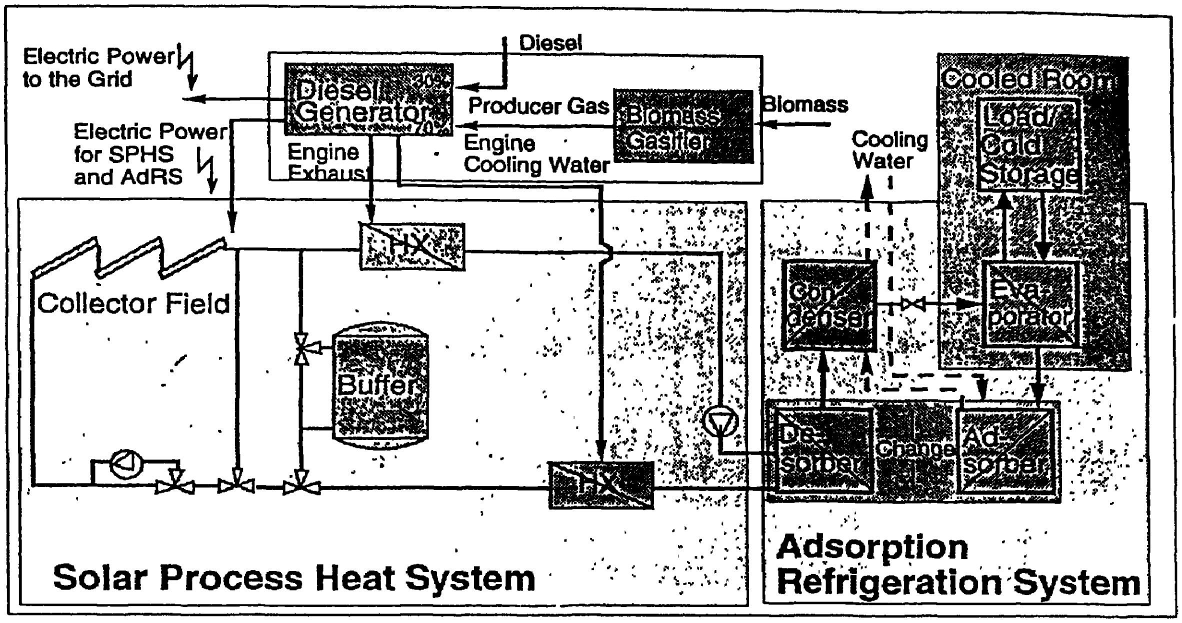


Figure 4.4: Draft system design for test plant

On the basis of the techno-economic study it has figured out, that it is more economical to run the system without auxiliary heater and to supply all additional heat by the waste heat of the genset. The additional electrical energy can be fed to the electrical grid (section 4.1.2). The system is depicted in Fig. 4.4.

In the modified system configuration the entire process heat demand is provided by solar and waste heat from the genset exhaust. For this purpose the diesel genset operating on dual fuel mode would be sized in such a manner that the waste heat recovered from its exhaust will be sufficient to meet the balance for the heat requirement (apart from that obtained by solar collectors). Though this increases the capital investment in gasifier based genset of higher capacity, selling the excess electricity produced (or its consumption for own purpose) generates income and in turn improves the economic viability by reducing the pay-back period.

The engine cooling water is limited to 85°C. Therefore it is more efficient to use the genset cooling water for heating up the adsorption cooling outlet. Otherwise in most operation modes the firing water would be cooled down in the heat exchanger by the cooling water.

A main effect of the use of the genset waste heat, thus is the rising of the collector inlet temperature by the heat exchanger for engine cooling water. The engine cooling water is about 85°C, which results in a collector inlet temperature of

about 80°C. For this reason, the collector outlet temperature is set to 85-90°C.

As there is no more auxiliary boiler there is the possibility of vaporization of water, when no heat is required at low storage loading. To avoid super heating two pressure relief valves are included to the system, which limit the water temperature to 100°C.

4.2.1 Economic Analysis

Capital cost reduction in %	Increase in price level in %	Pay back period for different collector areas in yrs 100 m^2	300 m^2	500 m^2
0	0	13.7	18.0	23.4
10	0	12.3	16.1	20.9
20	0	10.8	14.2	18.5
30	0	9.4	12.3	16.1
40	0	7.9	10.4	13.6
50	0	6.5	8.6	11.2
50	10	5.9	7.8	10.2
50	20	5.4	7.1	9.3
50	30	5.0	6.6	8.6
50	40	4.6	6.1	8.0
50	50	4.3	5.7	7.5
Genset capacity required in kW_e		110.1	102.9	95.7
Solar fraction in %		4.38	13.15	21.91

Table 4.4: Pay-back periods of alternative system configuration (for reduction in capital cost and escalation in price levels)

For collector area of 100 m^2 pay-back period is improved from 33.8 (first concept) to 13.7 yrs as the 110 kW_e genset provides 420859 kWh of surplus power generating additional income without much additional operating cost. Here the electricity selling price of 2.25 Rs/kWh is assumed which is the present accepted value for many state electricity boards in India. The results of the analysis for different levels of capital cost reduction and increase in price levels for 50% cost reduction are summarized in Tab. 4.4. It can be observed that with achievements of 50% reduction in system cost and with 50% increase in price level the pay-back period improves substantially to less than 5 years.

Using a compound parabolic concentrating collector (CPC) (η = 0.4) instead of a flat plate collector (η = 0.25) the pay back time can further be improved. Calculation for Tab. 4.5 are made with 34 kW_{th} VAdRS, CPC solar collector, COP_{VAdRS}=0.35.

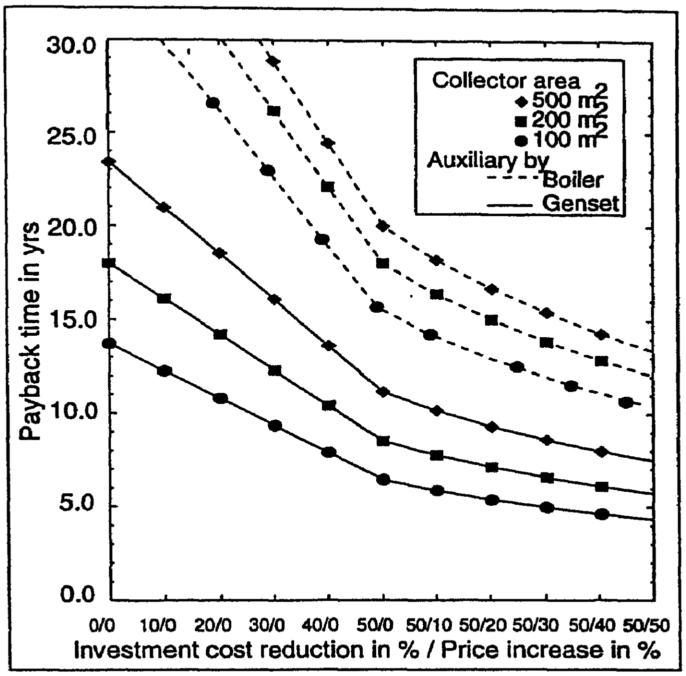


Figure 4.5: Economic analysis for cold store with 2000 T capacity

In the new system configuration, where only solar thermal heat and genset waste heat will be used to operate the VAdRS cooling unit. No auxiliary producer gas boiler will be used and extra electricity will be sold to the grid. It improves the pay-back period than the earlier configuration for this kind of technology. It has been observed that, CPC collector with higher efficiency level than flat plate collector has improved the optimization factor between solar fraction and capital cost of the solar collector. In the above table it has been clearly indicated that with the increase of solar fraction pay-back will be increased from 2.9 years to 6 years considering 50% capital cost reduction and 50% increase in price level. Higher the solar fraction lesser the carbon dioxide emission. So environmental cost benefit may encourage the increase in the solar fraction of this kind of system. But in the present circumstance, in the test plant it has been decided that 50% solar fraction will be maintained.

4.2.2 CO_2-Analysis

Solar-hybrid cooling systems will also address to global warming problem due to the use of non-CFC-based refrigerant and reduction in carbon dioxide emission due to increase in primary energy efficiency. Solar systems are zero emission technology as well as biomass system can also be turned into zero emission one through compensated afforestation. In this particular hybrid cooling system solar

Capital cost reduction in %	Increase in price level in %	Pay back period for different collector areas in yrs		
		100 m^2	300 m^2	500 m^2
0	0	8.9	13.5	20.4
10	0	8.1	12.1	17.9
20	0	7.1	10.8	15.9
30	0	6.2	8.4	13.9
40	0	5.3	8.1	11.9
50	0	4.4	6.7	9.9
50	10	4.0	6.1	9.0
50	20	3.7	5.6	8.3
50	30	3.4	5.2	7.6
50	40	3.2	4.8	7.1
50	50	3.0	4.5	6.6
Genset capacity required in kW$_e$		108	96	85
Solar fraction in %		3.7	14.86	37

Table 4.5: Pay-back period reduction with the reduction in capital cost and increase in price level using CPC-collectors

thermal collectors have been used with the thermal mix of waste heat of gasifier based power generation. In Fig. 4.6 carbon dioxide production in this solar hybrid cooling system has been plotted at different solar fraction.

Excess amount of generated power will be used by the near by community for their household purpose which means that amount of power is generated without generating extra amount of carbon dioxide.

This analysis has been done for a properly selected engine which can crater a heat requirement of a dedicated waste driven cooling system as well as solar-hybrid cooling system. At 20% solar fraction when diesel engine will be running in 74-75% loading of the engine diesel replacement dips down sharply and it dips the CO_2-emission of cooling also. It has been also observed that,with the increase of solar fraction production of CO_2 will be reduced due to the maximum use of solar thermal energy in the thermal form.

For comparison a conventional vapor compression system operated with electrical energy is also plotted. In this particular solar hybrid configuration cooling is simultaneously with the power generation. So in actual analysis the CO_2 production to generate the consumed electricity as well as the simultaneous power generation has to be considered.

For the CO_2 emission of the electricity production the average thermal mix of the Indian coal and grid is used with about 0.29 kg_{CO_2}/kWh_{el}, assuming 74% thermal mix in the Indian grid and 0.6-0.71 kg of coal/kWh_e. The COP for a

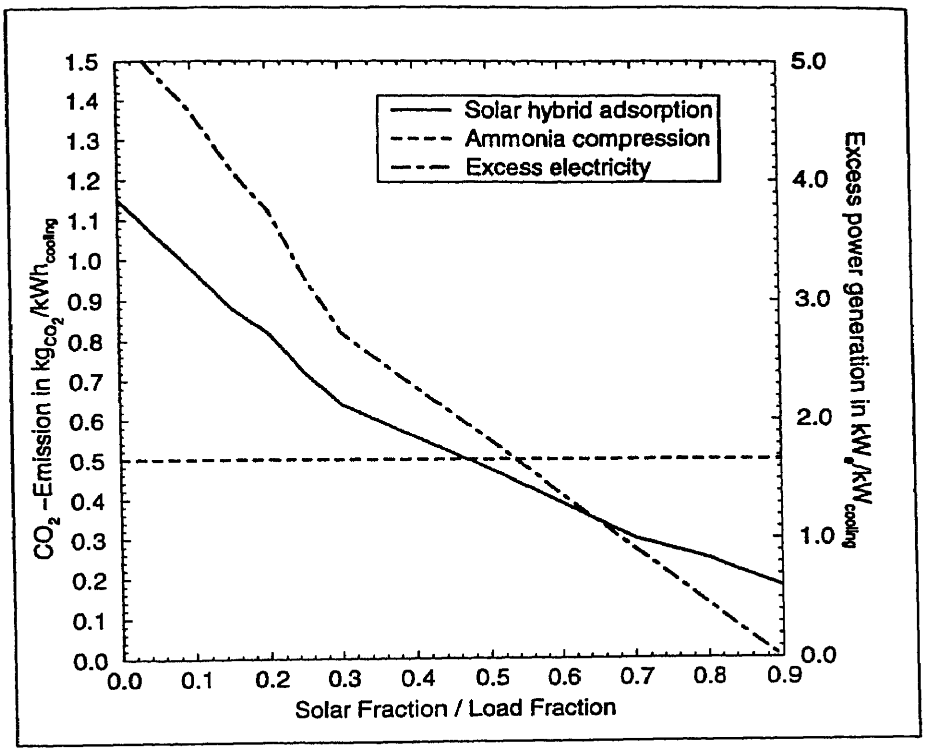


Figure 4.6: CO_2-Analysis for solar-biomass operated chiller

conventional ammonia compression system can be assumed about COP=2.1.

It clearly indicates that the specific CO_2-emission is around 0.5 $kg_{CO_2}/kWh_{cooling}$. In the solar hybrid cooling system using 50% solar fraction, which will be used in the test plant CO_2-production is also 0.6 $kg_{CO_2}/kWh_{cooling}$. So the configuration of the test plant is in the break even of the conventional and the solar-hybrid system as far as CO_2-production is concerned. It must however be mentioned that compensated afforestation or usage of agricultural waste as biomass fuel will reduce the CO_2-production significantly in the solar hybrid cooling system.

4.3 Parametric study

For a detailed system design a parametric study with a simulation model is carried out, to evaluate suitable system parameters by a parametric study.

Collector (flat plate)	Outlet set temperature	90°C
	Area	40 m^2
	Collector slope	28.6 °
	$F_R(\tau\alpha)_n$	0.74 W/m^2K
	$F_R U_L$	4.2 W/m^2K
Cold Store	Volume	80 m^3
	Cooling load and capacity according measured profile	
VAdRS	Nominal power (for water)	10 kW
	Cooling water temperature	29°C
	Mass flow cooling water	6 m^3/h
	Switch on temperature	-2°C
	Switch on radiation	500 W/m^2
Buffer Tank	Volume	5 m^3
	Height	3 m
	Total heat loss coefficient	1.44 kJ/hm^2K
Genset	Electrical Power	0.1-5 kW
	Exhaust temperature	350°C
	Exhaust mass flow	6.8 kg/kWh
	Cooling water outlet temperature	80°C
	Cooling water mass flow	90 kg/kWh
	Exhaust HX efficiency	0.9
	Cooling water HX efficiency	0.9

Table 4.6: Parameters for the TRNSYS-simulation

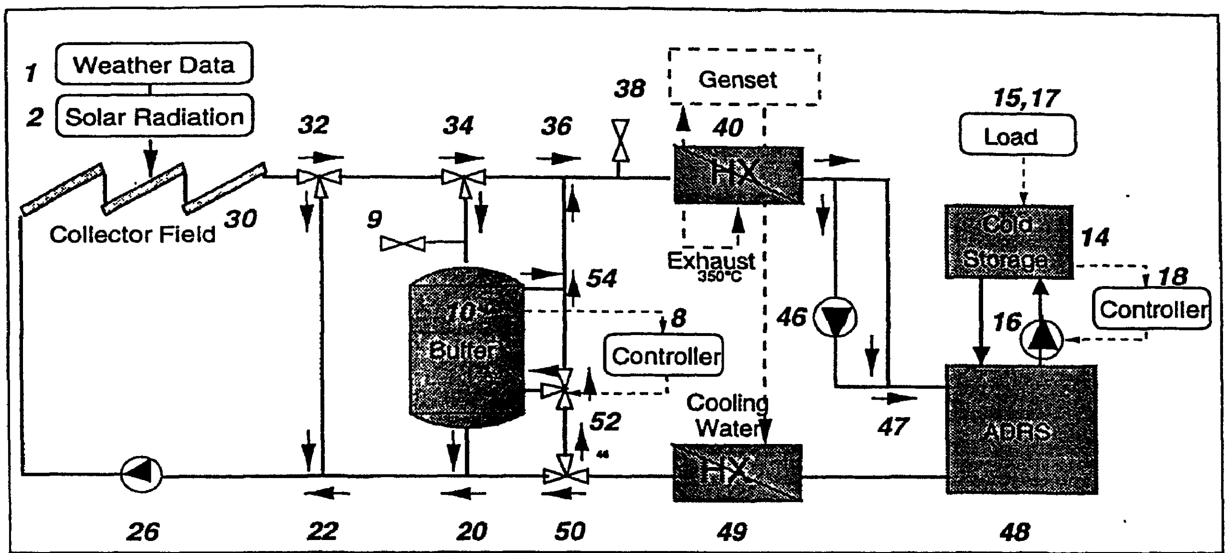
4.3.1 System model of the modified concept

With the results of the first concept the preliminary system is modified. The most important change is to remove the auxiliary boiler and to increase the genset capacity. By this the engine heat can be used to meet the additional heat demand.

Due to the heating up of the outlet water of the chiller by the genset cooling water the operating temperature level of the collector field raises. To reach furthermore good results a flat plate collector using compound parabolic concentrator (CPC) is used instead of a normal flat plate collector.

In addition the tank model is changed, due to the errors, which has been found in the TRNSYS standard type.

The resulting simulation deck is displayed in Fig. 4.7 and the source code is given in the appendix B.



Unit	Component	Unit	Component
1,2,15,17	Data Input	20,22, 36, 47, 54	T-Piece
8,18	Controller	30	Collector
9, 38	Pressure relief valve	32, 34 ,45, 50, 52	Flow diverter
10, 14	Storage tank	40, 49	Heat exchanger
16,26,46	Pump	48	Adsorption cooling system

Figure 4.7: Scheme of the modified simulated system

4.3.2 Parameter variation

A parametric study has been done, to determine adequate component parameters. Basing on the evaluated load profile and the meteo-data of a cold storage near Delhi (section 2) simulation are carried out

In Fig. 4.8 the yearly solar fraction, defined by

$$F = \frac{Q_{coll,u}}{Q_{coll,u} + Q_{HX,cw} + Q_{HX,gas}} \quad (4.1)$$

is displayed as a function of the buffer tank volume for different sizes of the collector area. From this evaluation follows, that there is a relation between between collector area and optimal buffer tank volume.

In Fig. 4.9 the collector field area is varied using the optimal buffer tank volume for the different collector field sizes from the former parameter variation. The result shows, that due to the high losses of the oversized collector field even in the summer months the yearly solar fraction will be lower, as displayed in Fig. 4.8. By this can be deducted, that the collector field shouldn't be larger than 40 m^2 to avoid high losses by over-heating.

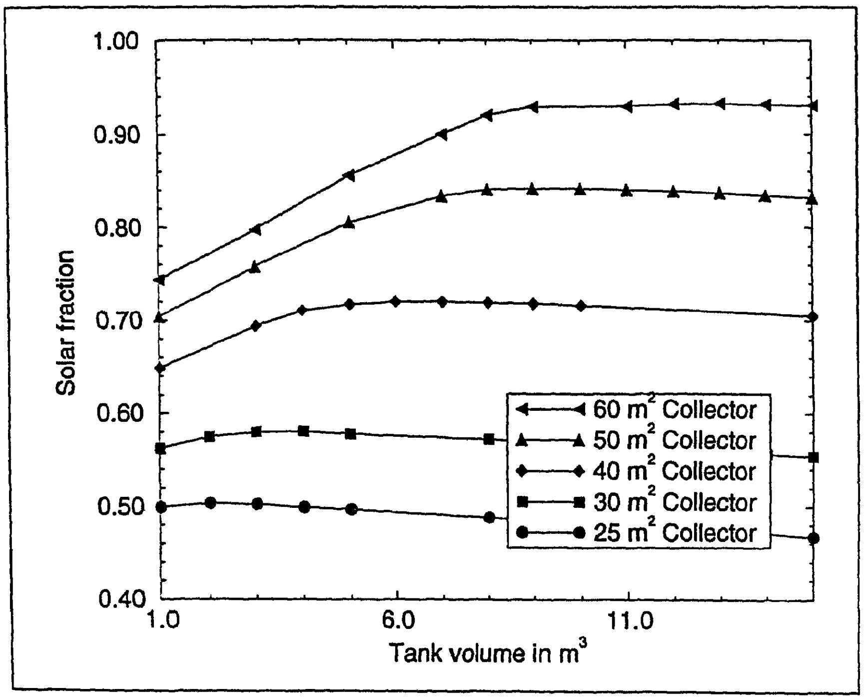


Figure 4.8: Effect of tank volume on solar fraction

In the yearly profile for genset can be seen, that the maximal electrical output, resulting from the heat requirements in the exhaust heat exchanger is about 2kW. A genset with a capacity of about 3-5 kW_{el} therefore is sufficient.

The results of a yearly simulation with the parameters given in Tab. 4.7 are shown in Fig. 4.10.

With the given system it is possible to keep the storage room temperature below 2°C. In July and August (4320-5760 h) there are some peeks in the temperature, which nearly reach the upper limit. These days are rainy days according to the weather data with low radiation. Together with the small capacity of the partly loaded storage this results in a quick rising of the temperature.

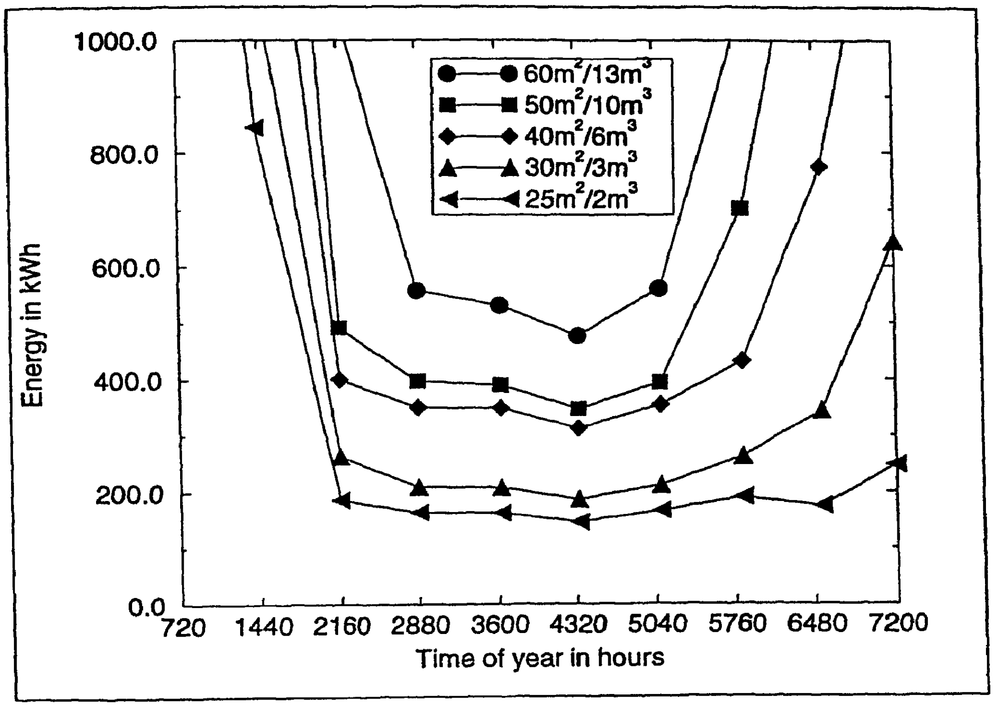


Figure 4.9: Effect of collector field size on boiling losses

Collector (ETC)	Outlet temperature	85°C
	Power (average)	4.8 kW_{th}
	Power (peak)	19 kW_{th}
	Area	40 m^2
Buffer tank (volume)		5 m^3
Cold storage	Volume	240 m^3(100t)
	Temperature	3/-2 °C
	Average cooling load	3.5 kW
Adsorption cooling machine	Nominal capacity	10 KW_{th}
	COP	35%
Genset	Power (electric)	5 kW_{el}
	Amount of waste heat (η_{HX}=80%)	8 kW_{th}
Solar fraction		50%

Table 4.7: Design parameters of the modified solar-hybrid adsorption cooling system

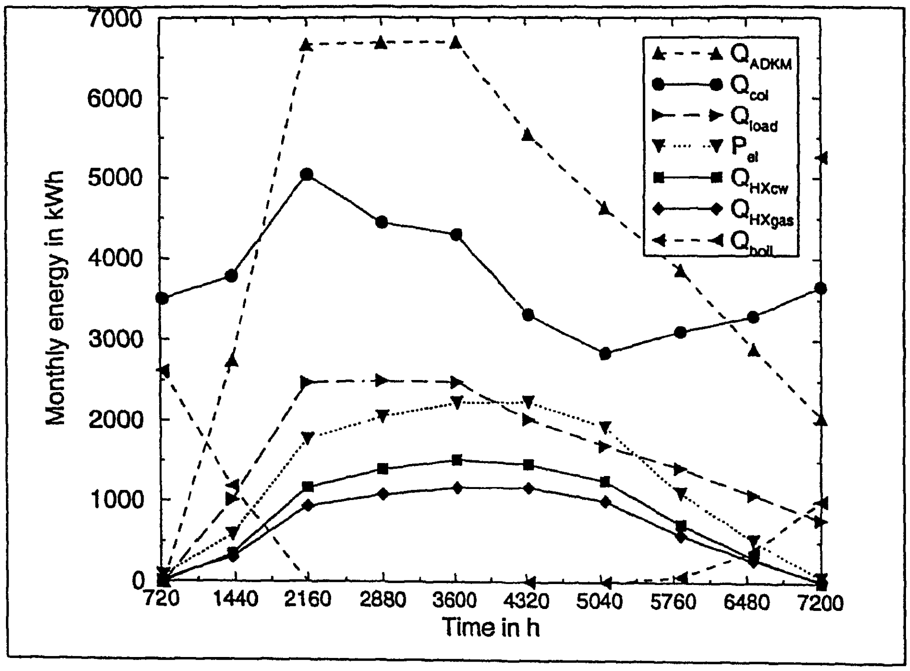


Figure 4.10: Monthly energy amounts of the system components ($A_{col} = 40$ m^2, $V_{tank} = 5$ m^3)

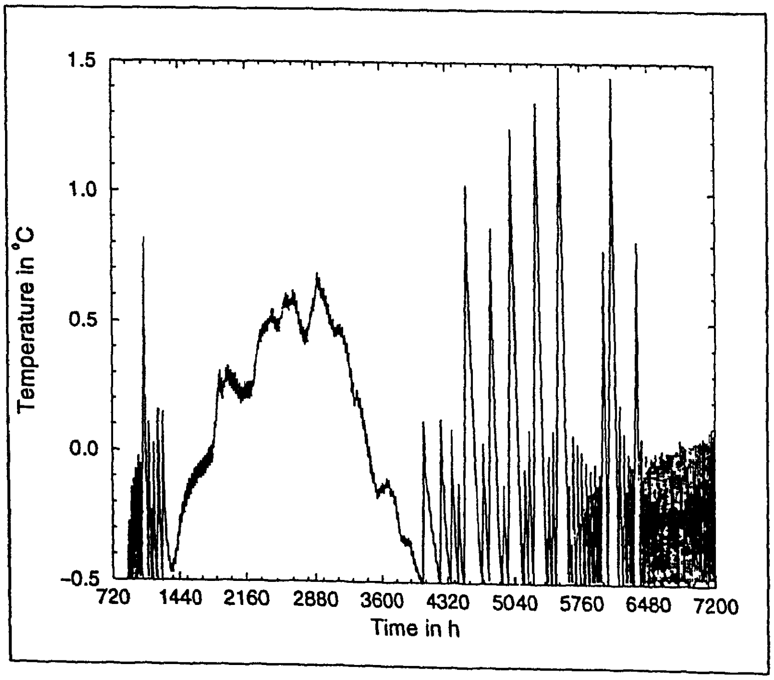


Figure 4.11: Cold storage room temperature ($A_{col} = 40$ m^2, $V_{tank} = 5$ m^3)

Chapter 5

Draft design of test plant

According to the results of the system analysis a draft design for the test plant is carried out by TERI and DLR. The relevant parameters for the system components are given as overview in Tab. 5.1.

Cold storage	Volume	240 m^3 (100 t)
	Temperature	3/-2 °C
	Average cooling load	3.5 kW
Adsorption cooling machine	Effective capacity	10 kW_{th}
	COP	35%
Cooling tower	Power	18 kW_{th}
Gasifier	Power	20 kW_{th}
Genset	Power (electric)	5 kW_{el}
	Amount of waste heat (η_{HX}=80%)	8 kW_{th}
Collector (CPC)	Outlet temperature	85°C
	Power (average)	4.8 kW_{th}
	Power (peak)	19 kW_{th}
	Area	40 m^2
Buffer tank	Volume	5 m^3
Solar fraction		50%

Table 5.1: Draft design parameters for the test plant (100 t potatoes)

A draft system design is carried out for this parameters resulting in the components, which are described in the following section.

5.1 Cold store

5.1.1 Location

In the second phase of the project a cold storage prototype of 240 m^3 capacity will be constructed in TERI's Gual Pahari campus, 25 km south from New Delhi.

5.1.2 Building

The design of the cold store is based on the down scaling of the Hapur cold stage dimensions (Tab. 5.2).

Volume:	240 m^3 for 100 t / 1250 bags potatoes
Size:	9 × 7 × 3.8 m (9 m length side is facing east) Actual height 2.4 m, remaining 1.4 m will be used to place air handling, duct etc. wooden strips with 1"gap, in short no rigid partition).
Wall:	36cm thick brick wall (with outside plaster), 390 mm thick rice husk insulation layer from inside, 100 mm thick inner brick wall No plaster inside.
Roof:	Concrete slab (100 mm thick) outside, 230 mm air gap on inner side between concrete slab and 390 mm thick rice husk layer above asbestos cement sheets (2-3 mm thick).

Table 5.2: Cold storage chamber details

5.1.3 Cooling coil

A pure brine-air cooling coil is preliminary designed as cross flow heat exchanger according to ASHRAE[1]. The coil is placed on the top of the cold storage. A two row plate fin type cooling coil has been selected where entering brine and air temperature are -2°C and 3°C and brine and air outlet temperatures are respectively 2°C and -1°C. The linear mean temperature difference in this cross flow tube is 3.6°C. Total heat exchange surface area is 47 m^2 with a primary and finned surface area ratio of 20. Actual dimensions of the coil tube and fins will be selected according to the manufacturers data. Required air flow rate is 1.5 m^3/s (3200 ft^3/min). Two forward curved centrifugal fans have been selected which will supply the required amount of air and generate a pressure drop of 390 Pa to balance the draft in the air handling system. A rectangular shaped insulated duct with an equivalent circular diameter of 450 mm and actual dimension (667 × 267

mm) has been selected which will allow the cooled air in the cold storage room with an approach velocity of approximately 2 m/sec.

Flow mode	cross flow
Brine inlet temperature	-2°C
Brine outlet temperature	2°C
Brine mass flow	1.5 m^3/h
Air inlet temperature	3°C
Air outlet temperature	-1°C
Air mass flow	1.5 m^3/s
No of parallel fans	2
Air pressure drop	390 Pa
Linear mean temperature difference	4 K
Bare tube area (brine)	2.35 m^2
Total area (air)	47 m^2
Ratio of total to bare tube area	20

Table 5.3: Cooling coil design

5.1.4 Stored goods

For results very close to later operation generally potato will stored in this cold storage simulator. However if potatoes are not easily available green wood can also be stored alternatively, which is much cheaper and has nearly the same thermal behavior.

5.2 Cooling system

For the use with solar collectors and genset waste heat a sorption system is most suitable. Due to the low driving temperature an adsorption system is chosen.

5.2.1 Adsorption cooling system

Up to now there is only one commercial system operating with the water/silicagel available on the market. The technical data for the smallest unit are given in Tab. 5.4.

According to the German company it is planed to produce a smaller system with about 20 kW nominal power until end of 1996. Operating this with the refrigerant methanol, the power range should meet the demands of this project. The

Firing water loop	Inlet temperature	85 °C
	Outlet temperature	79.4 °C
	Temperature difference	5.6 °C
	Volume flow	18 m^3/h
	Firing energy Q_h	118 kW
Chilled water loop	Inlet temperature	14 °C
	Outlet temperature	9 °C
	Temperature difference	5 °C
	Volume flow	12 m^3/h
	Chilling capacity Q_0	71 kW
COP (Q_0/Q_h)		0.6
Required Cooling water power		189 kW
Cooling water loop	Inlet temperature	31 °C
	Outlet temperature	34.8 °C
	Temperature difference	3.8 °C
	Volume flow	42 m^3/h
Measures and weights	Length	3370 mm
	Width	1600 mm
	Height	1600 mm
	Running weight	5000 kg
	Transportation weight	4000 kg

Table 5.4: Technical data of commercial adsorption chiller [3]

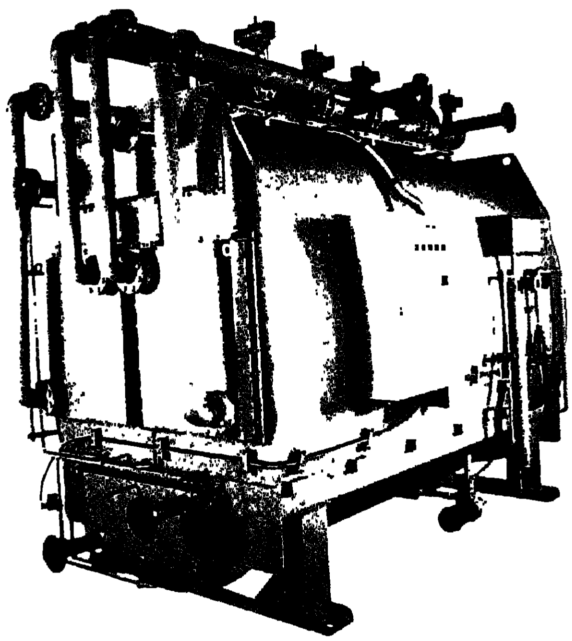


Figure 5.1: Adsorption chiller NAK 70 kW [3]

operating conditions have to be modified according to the experimental results, given in section 5.2.1. By lowering the outlet of the chilled loop, instead of water brine has to be used, to prevent freezing. The design parameters for the modified adsorption chiller are given in Tab. 5.5.

For the sorption cooling system a cooling tower is required, to remove the waste heat at the required cooling water temperature level. For the cooling water power is about 4 times the chilled water power, due to a COP of about 35%.

5.2.2 Cooling tower

An induced draft air cooled cooling tower is selected to remove the heat from condenser cooling water. Range and approach of this cooling tower is 4 K and 8.9 K where wet bulb temperature is 21.1°C. Water flow rate is 1.1 kg/sec. Cross sectional area of the cooling tower is 0.9 m^2. Considering 90% of rated design fan power consumption will be 0.229 kW_e. Height of this mechanical drafted

Firing water loop	Inlet temperature	85 °C
	Outlet temperature	75 °C
	Temperature difference	10 °C
	Volume flow	1.2 m^3/h
	Firing energy Q_h	14 kW
Brine loop	Inlet temperature	2 °C
	Outlet temperature	-2 °C
	Temperature difference	4 °C
	Volume flow	0.9 m^3/h
	Chilling capacity Q_0	3.6 kW
COP (Q_0/Q_h)		0.3
Required Cooling water power		18 kW
Cooling water loop	Inlet temperature	30 °C
	Outlet temperature	34 °C
	Temperature difference	4 °C
	Volume flow	4 m^3/h
Measures	Not known yet	

Table 5.5: Technical data of modified adsorption chiller using methanol

cooling tower depends upon the mass transfer area of the fill and it will be finalized according to the manufacturer specification. Cooling tower characteristics (water/air flow) for this cooling tower is approximately 1.25.

5.2.3 Brine

Due to the cooling temperature below the freezing point of water a brine has to be used for the heat transfer fluid. The temperature range of operation is between -5°C and 30°C at shutdown.

For this temperature range e.g. 10% ethylenglycol or 15% 1,2-propylenglycolether can be added to the water prevent freezing at -5°C. Freezing protection based on ethylenglycol results in better thermodynamic properties than propylenglycolether, whereas propylenglycolether is not critical for use in food sector. In Tab. 5.6 the material properties are given for commercial products, which also have corrosion inhibitors added. Full corrosion protection is reached with 20% Antifrogen N or 25% Antifrogen L.

These glycol based freezing protections can also be used in the collector loop, if necessary. Operating temperatures above 95°C however might cause problems, due to evaporation.

Antifrogen	Type N		Type L	
Volumetric fraction in %	10	20	15	25
Corrosion protection Yes/No	N	Y	N	Y
Freezing point in °C	-4.9	-10.4	-4.8	-10.1
Boiling point in °C at 1013 hPa	102	103	101	102
Density in g/cm^3	1.02	1.04	1.02	1.03
Kinematic viscosity in mm^2/s	2.64	3.76	3.93	6.55
Specific heat capacity on kJ/kg K	4.1	3.89	4.15	3.93
Heat conductivity in W/mK	0.539	0.507	0.506	0.468
Heat transfer relation (based on H_2O at 20°C)	0.58	0.47	0.47	0.35

Table 5.6: Physical properties of Antifrogen at -2°C [5]

5.3 Biomass system

The gasifier system to be coupled to the diesel genset consists of (i) fuel processing unit, (ii) main gasifier, (iii) gas cleaning/cooling train and (iv) waste utilization unit. These are described briefly below.

5.3.1 Gasifier

The fuel processing system is designed so as to process most biomass residues. The different routes for biomass processing are shown in Fig. 5.2.

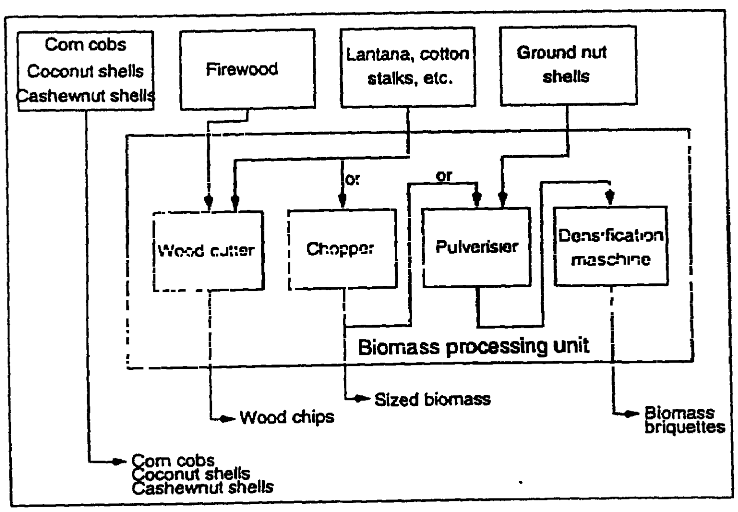


Figure 5.2: Routes for biomass processing

It consists of a wood cutter, a chopper, a pulverizer and a ram and piston type briquetting (densifying) machine. The wood cutter is primarily used for cutting

long pieces of wood into smaller ($\approx 5 \times 10$ cm) pieces, which are desirable as they ensure smooth fuel flow within the gasifier thus avoiding bridging. Agricultural residues like corn cobs, coconut shells, cashewnut shells etc. can be used directly without any preprocessing. Residues like mustard stalks, cotton stalks, lantana etc. can be chopped and used directly, provided they have a reasonably good bulk densities ($\approx$250 kg/m^3). The chopper is a conventional chaf cutter extensively used in rural areas for fodder cutting. Biomass residues such as groundnut (peanut) shells will have to be pulverized and then densified. The pulverizer is a conventional hammer mill grinder available easily in the market. Items like saw dust can be directly briquetted. The briquetting machine is a commercially available ram and piston type; which has gained popularity and commercial acceptance in recent years. These units will use some of the power generated by the power plant, but as they are not used simultaneously, they do not draw heavy load. The electricity consumption for the various biomass processing units is in the range of 0.02-0.1 kWh/kg.

Type	Downdraft, throat-less
Specific gasification ratio	0.1 Nm^3/cm^2 hr
Gas production	2.3-2.5 Nm^3/kg
Gas calorific value	4200-5000 kJ/Nm^3
Cold gas efficiency (energy in gas/energy in biomass)	70-78%

Table 5.7: Technical details of gasifier (gas data for normal conditions)

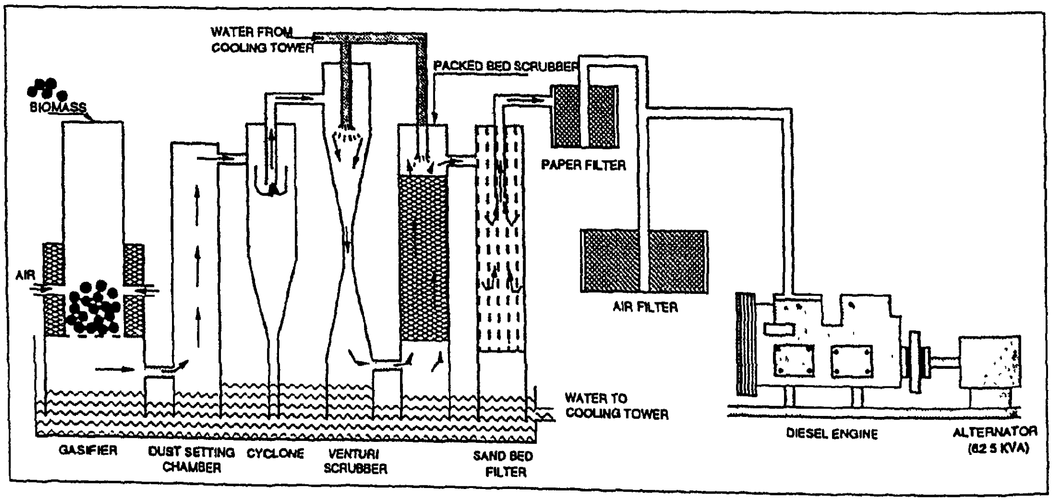


Figure 5.3: Schematic diagram of the gasifier based power generation set up

The main gasifier is a downdraft throat-less design with a low specific gasification rate and provided with a continuous char removal system. It consists of

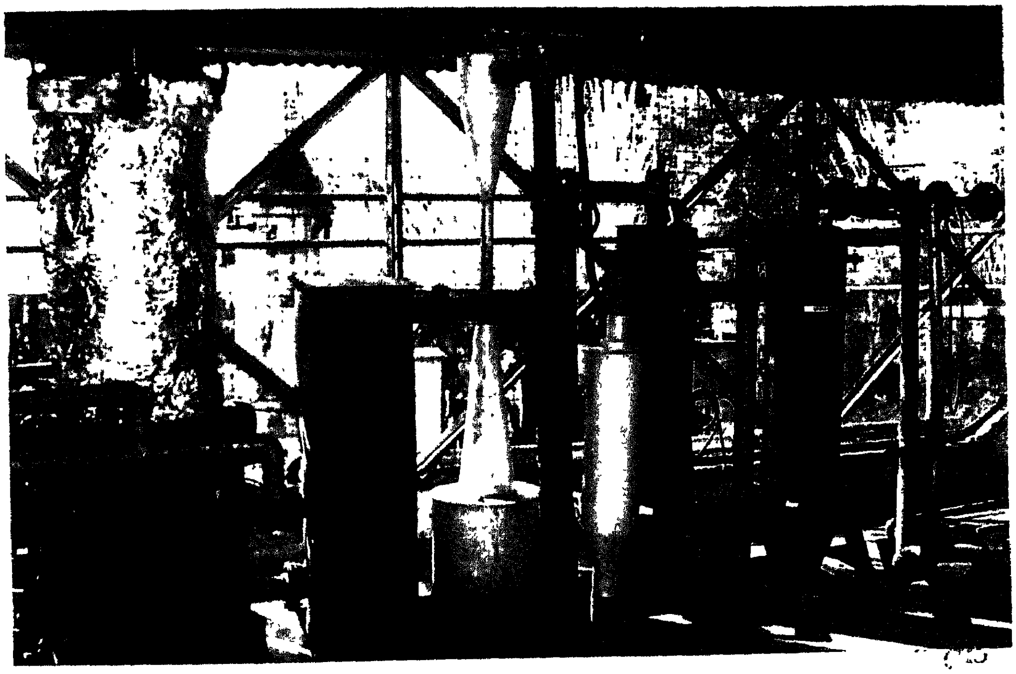


Figure 5.4: TERI biomass gasifier (40 kW)

a fuel hopper (storage bin), the reaction zone, a vibrating grate, all provided in a integral unit. In its travel through the gasifier, biomass drying and oxidation (combustion) undergoes followed by conversion to producer gas and char. The char is collected in a water pond below the grate and the gas is taken out through a bottom side port for further cleaning. Fuel is charged from the top through a gas-tight port, which is opened and closed manually. The storage bin accommodates sufficient fuel for a 2 hour operation at full load. However, as the gasifier is under slight vacuum, fuel can be changed at frequent intervals without interrupting gas production or power generation. Two air nozzles are provided for combustion. The technical details of the gasifier are listed in Tab. 5.7.

The raw gas contains appreciable amounts of tar and solid particulate matter, to the tune of 1500-2000 ppm. The impurity levels should be reduced to about 50 ppm before admitting the gas into any internal combustion engine. This is achieved by passing the gas through a series of units viz., a gravity settling chamber, a cyclone, a venturi scrubber, a packed bed scrubber, a sand bed filter and a paper filter, as shown in Fig. 5.3 and 5.4.

By the end of cooling/cleaning train, the producer gas is at ambient temperature and the total impurity content is down to 30-50 ppm. The water used for cleaning/cooling is recycled after screening for solid particles, and passing through a natural draft cooling tower.

The principle waste produced is biomass char and the tar and particulate matter collected while cleaning the gas. The gasifier is designed so as to produce char and not ash. The char and other solid matter collected in the water tanks is mixed and allowed to sun-dry for a day or two. After this it was fed to a low pressure screw extruder for making char briquettes. Analysis of these briquettes showed that they contain 50% carbon, 40% ash and minor quantities of hydrogen and nitrogen. The calorific value of the briquettes was in the range of 14500-16500 kJ/kg. The briquettes are thus suitable for sale as solid fuel to commercial enterprises like road side hotels.

5.3.2 Genset

The complete power plant

Gas produced from biomass as described above, is fed into a suitable diesel genset. The capacity and specifications of the genset are selected a-priori and the capacity of gasifier and other sub- systems are designed in accordance. For example, for a 62.5 kVA genset with 6 cylinders of swept volume 6.614 liter and 1500 RPM, the gasifier will have to be designed to consume about 50 $kg_{biomass}/h$. The producer gas, when burnt inside the diesel engine along with diesel oil, will replace up to 70% of diesel. The diesel replacement figures for a 50 kW gasifier power plant are shown in Fig. 5.5 for different fuels.

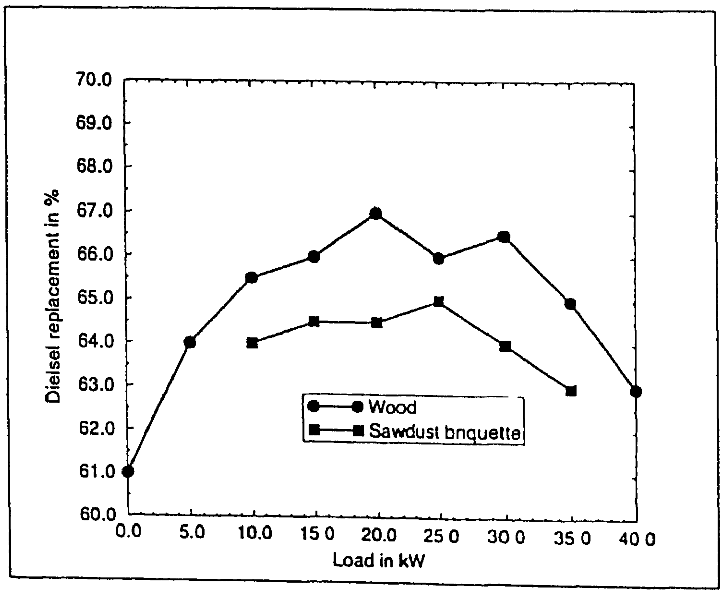


Figure 5.5: Diesel replacement achieved with dual fuel mode operation of diesel genset

On a continuous basis, the power plant consumes about 108 ml diesel and 1.1 kg biomass to produce 1 kWh of electricity. Out of this, about 10% is used for parasitic consumption and the result is available either for feeding into the grid or for captive utilization.

Gasifier coupled dual fuel engine

Water cooled 30 kVA (Model name: Kirlosker RBOO) diesel generator set will be converted to a biomass gasifier based dual fuel engine considering average loading of 50%.

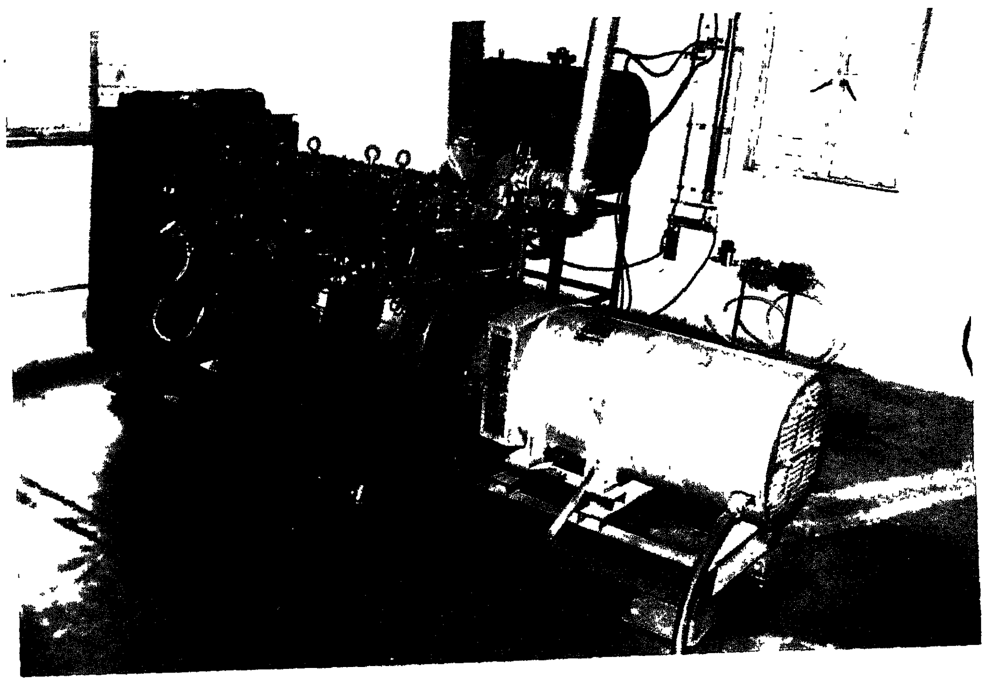


Figure 5.6: TERI producer gas operated diesel genset (30 kVA)

5.4 Collector field

The collector field has to be designed appropriate to the solar cooling application. Due to the adsorption chiller, the collector temperature will range between 80-100°C. With ambient temperatures 20-40°C the resulting temperature difference will be about 50-70 K.

The present state of collector technology for solar cooling application is recently been screamed in a study for the European Commission by Pereira et al [11]

5.4.1 Collector technology

For the major types of collectors typical efficiency curves are given in Fig. 5.7. From this figure can be derived, that for the working conditions of

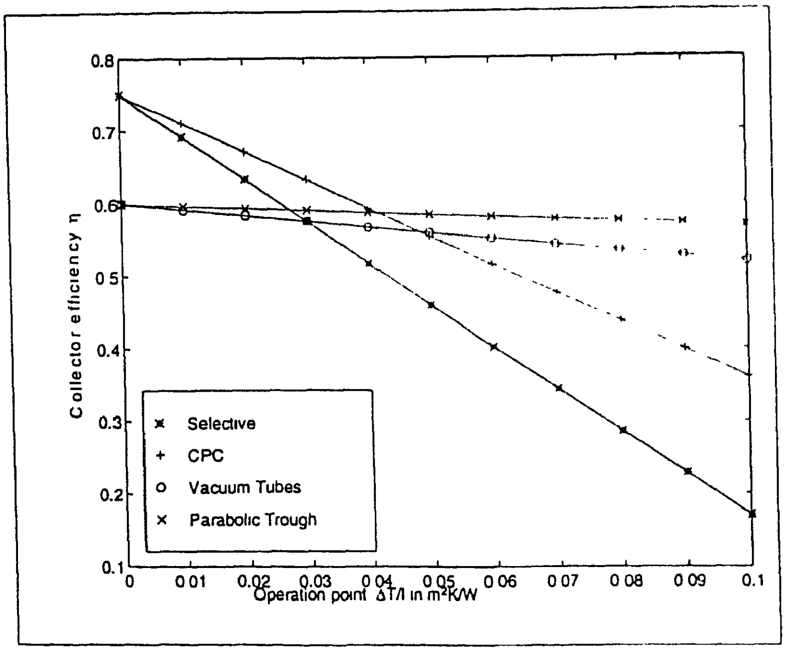


Figure 5.7: Efficiency comparison of different collector types

$$\Omega = \frac{\Delta T}{I} \approx \frac{50 - 70\text{K}}{500 - 1000\text{W/m}^2} = 0.05 - 0.14\text{Km}^2/\text{W} \tag{5.1}$$

flat collectors have obviously much lower efficiency than evacuated tube (ETC) or compound parabolic concentrator (CPC) collectors. For $\Omega > 0.06$ m^2 K/W parabolic trough collector have the highest efficiency. For economical reasons CPC seems to be mostly recommended. In Tab. 5.8 the specific cost for 1kW thermal power at $\Omega = 0.8$ m^2 K/W for different systems is given.

Collector Type	Collector Price in ECU/m^2	Efficiency η	Power price in ECU/kW
Flat-Plate	130 - 400	0.3	540 - 1650
CPC	165 - 300	0.45	450 - 825
ETC	650 - 1170	0.6	1350 - 2430
Parabolic Trough*	160	0.8	250

Table 5.8: Specific cost of current collectors at $\Delta T = 58$ K and $I = 800$ W/m^2
*: Price is only available for large collector fields

The calculation is based on the average collector price in Europe a temperature difference of $\Delta T = 58$ K and global radiation $I = 800$ W. The cheapest non tracking system under this condition seems to be CPC, with cost of about 660 ECU/kW.

Only the costs for parabolic trough collector with 250 ECU/kWh are lower, than those of CPC. The collector price for parabolic trough collectors however is calculated on the basis of large collector fields for solar power plants. The costs for small installations will be much higher, as all the control equipment has a fixed price. In spite of the low specific costs tracking systems seems not to be appropriate, as they need more service due to the moving parts and for cleaning the mirrors. Additionally the price apply to large fields. By the fixed costs small systems would be more expensive.

5.4.2 Control

The driving temperature depends on the chiller characteristics and varies with the load. If the use of auxiliary energy is to be minimized the temperature of the supplied heat should match the requirements of the cooling process. Thus it is necessary to use a temperature control that adjusts a certain collector outlet temperature and keeps it in spite of variations in the irradiance.

Commonly the flow rate is used as manipulated variable only. Utilizing the load bypass operation as an auxiliary manipulation can enlarge the adjustable range of outlet temperatures and enable an automatic plant operation. Hence a suitable control structure is required to coordinate the manipulations.

This control strategy, described in the following section has been proven in a test plant for solar process heat[8]. the principle of control is suggested by Zunft[14].

Structure of the Control System

A fast temperature control can be obtained by manipulating the mass flow in the collector loop. As the mass flow is subjected to constraints only a small range

of outlet temperatures can be adjusted. This can easily be seen in steady state considerations. A continuous load bypass operation can enlarge this range of adjustable temperatures. Its disadvantages are the unfavorable dead time behavior in the system response and the increased losses due to the higher temperatures in the supply pipe. These disadvantages have to be moderated by an appropriate control structure. The chosen structure is depicted in Fig. 5.8.

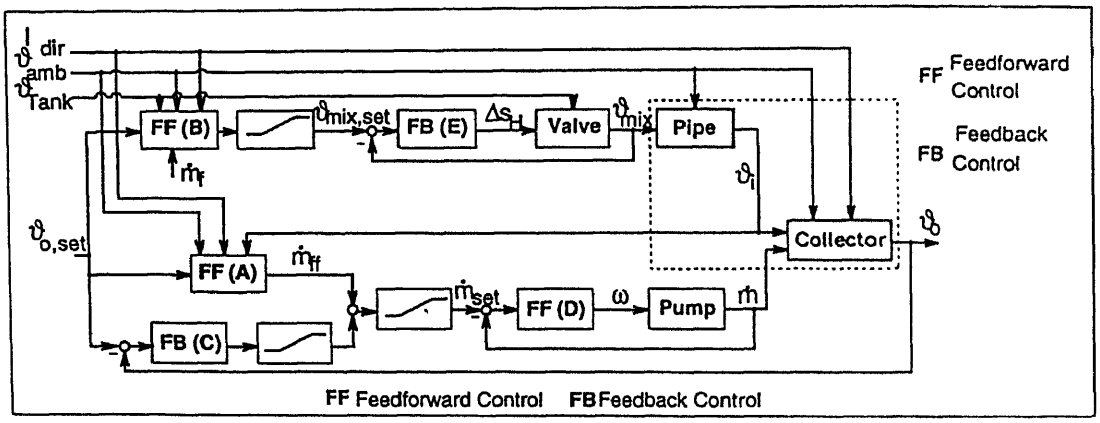


Figure 5.8: Collector outlet temperature control structure

The main features of the structure are i) the integration of model knowledge to achieve a fast control and ii) the unambiguous assignment of the two manipulating variables $\dot{m}$, ϑ_{mix} for one given set point of the collector outlet temperature $\vartheta_{o,set}$.

The main manipulating variable $\dot{m}$ is the combined output of a feed-forward(A) and a feedback (C) controller. The feed-forward control (A) contains a distributed steady state model of the collector and calculates the mass flow required to reach the desired outlet temperature $\vartheta_{o,set}$ from the online-measured irradiance E_{dir}, ambient temperature ϑ_{amb} and the collector inlet temperature ϑ_i. Disturbances can be compensated by the feed-forward controller before their effect on the collector outlet temperature is noticeable, thus resulting in a fast controller response. The remaining set point deviations arising from model inaccuracies are measured and reduced by the parallel feedback controller (C) with PI-characteristic. The mass flow is adjusted by the pumps motor speed ω. To keep away disturbances in the mass flow regulation from the main control loop, a cascaded control (D) is used for this purpose.

The use of a feedback controller with the auxiliary manipulated variable would lallow only small controller gains. Therefore a pure feed-forward control (B) containing the distributed steady state model of pipe and collector is used. The valve outlet temperature ϑ_{mix} is regulated by a cascade control acting on the valve's lift s. The remaining set point deviations are reduced by the main manipulating variable.

The use of the two manipulating variables has to be coordinated in a way that the auxiliary manipulated variable is only used when the main manipulated variable approaches its minimum value $\dot{m}_{min}$. This is achieved by using a constant mass flow value $\dot{m}_f$ instead of the measured value as an input in feed-forward unit (B). As the result a measured mass flow dropping below $\dot{m}_f$ causes the valve inlet temperature to be raised , i.e. a continuous bypass operation to be performed. The valve's outlet temperature is adjusted such that the collector outlet temperature can be reached with $\dot{m} = \dot{m}_f$ in steady state conditions. A measured mass flow greater than $\dot{m}_f$ causes the valve to be closed, i.e. no bypass operation to be performed. If $\dot{m}_f$ is chosen slightly above $\dot{m}_{min}$ the remaining set point deviations can be reduced by the feedback controller (C).

5.5 Auxiliaries

5.5.1 Piping

Centrifugal monoblock pumps will be used for all the pumps except hot water and brine pump. Temperature controlled two way valve will be used for the hot water circuit. For all hydraulic it is important to keep pressure in the piping small, to reduce parasitic power consumptions.

5.5.2 Buffer Tank

A cylindrical hot water storage of 5000 kg of water will be used. Diameter and height of the tank are 1.7 m and 2.2 m respectively. The tank will be made of steel plates. Angles etc. will be used to strength the body of the tank and it will be insulated all around with glass wool insulation of 20 cm thick. Pressure regulated steam vent will be provided for safety.

5.5.3 Operation strategy

The operation strategy is dominated by the basic problem of solar operated sorption cooling systems. The collector efficiency raises as operating temperature goes down, where as the sorption system prefers higher operating temperatures (Fig. 5.9). Thus it is aspired to operate the heating loop as close as possible at an optimum temperature, which is for this application at about 90°C. Using the waste heat of the biomass genset the collector inlet temperature is limited by the cooling water heat exchanger to about 80°C. With a temperature drop of 10-12 K in the chiller the heating water inlet should be 85-90°C. With an additional genset exhaust heat exchanger a temperature lift of about 3°C of the collector

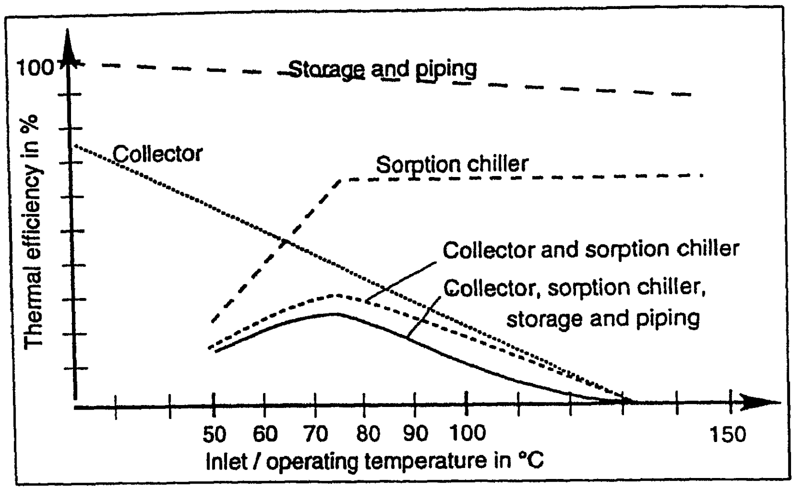


Figure 5.9: Correlation of the performance of system components

outlet is achieved. By this limitations the collector outlet temperature is set to about 85°C. As described above, this can be achieved by a mass flow control. If the solar gain is not sufficient and chiller inlet temperature is two low the heating water temperature can be regulated by the genset exhaust. Operating the genset at a higher power level, more waste energy is produced, which heats up the firing water.

As far as possible the plant is operated with minimum auxiliary input, to achieve maximum solar gain. By the buffer tank it is possible to store surplus solar energy for a short time to run the system for a longer period with out rising the genset power level. Thus the genset can be operated after reaching a sufficient insolation (about 500 W/m^2) with the genset running on the minimum level, producing just the required energy for plant operation. Only in night and morning time additional energy by the auxiliary is needed.

If more electrical power than waste heat is needed for a short period, the chiller can be operated on higher level and the energy directly used to cool down the store within the acceptable temperature range. The priority however is not to provide electrical power, but to achieve better economic viability by genset waste heat driven system.

Chapter 6

Summary and Conclusions

6.1 Results from phase 1

In this first phase of the project, which is conceived with 2 phases, the basis for the design and construction of a solar-hybrid adsorption cooling system is established.

In the first step all data, which are necessary for the design of the solar-hybrid cooling system have been collected. Meteo data, as well as the load profile of an existing potato cold storage are now available.

Based on these data a draft system design has been carried out. Due to the constraints of the operation temperature level an adsorption chiller seems to be the most suitable cooling system. A commercially available system for air-conditioning application has to be modified for the operation at cooling temperature below the freezing point of water. Methanol instead of water can be used as refrigerant. Because of the inferior thermodynamic properties and the lower operation temperature the efficiency will be reduced. Experiments and calculations show, that the COP will be about 30% when operating the system with methanol/silicagel at a chilled water temperature $T_0 = -2°C$, a heating water temperature of $T_h = 85°C$ and a condenser temperature $T_c = 30°C$.

The initial system parameters have been optimized using numerical system simulation with the aid of the TRNSYS-package. Due to the limited temperature drop in the adsorption chiller and the use of the genset waste heat, the collector field is operated at a high temperature level of about 85°C. Therefore it turns out, that it is more economical to use CPC-collectors instead of simple flat plat collectors. The better efficiency of the CPC-collector at the point of operation compensates the price advantage of flat plat collector.

Furthermore the calculation shows, that there is an optimal size for the buffer

tank, depending on the collector filed size. For about 40 m^2 of collector a buffer tank with 5 m^3 seems to be most suitable. If the tank is smaller, the solar fraction goes down because surplus energy cannot be stored. If the tank is larger, the solar fraction goes down, because the solar input is to small to heat up the tank to operation temperature of the chiller.

Economic analysis shows, that operating the system with a solar field and a biomass boiler as auxiliary heater results in very long pay back times of 10-40 years, depending on the economical boundary conditions. However firing the boiler with the waste heat of a generator and not using biomass directly results in much better economic data. The additional revenues obtained by selling electricity produced by the biomass fueled generator decreases the pay-back period by 50%.

With the results of simulation and economic analysis a draft design for a 100 t potato cold store at the TERI-campus in Gual Pahari, close to Delhi is elaborated.

6.2 Work package for phase 2

The overriding objective of the second phase of this joint research project is to test, to evaluate and to demonstrate an advanced solar hybrid adsorption cooling system by a pilot plant in India.

A test site at the TERI-campus seems to be appropriate, since all the experimental and technical infrastructure as well as also rural conditions for a realistic test operation are available.

Presently there is no commercial system available operating with methanol/silicagel, therefor the water/silicagel system will be modified for the operation with methanol as refrigerant and will be tested.

After setting up the cold store on the campus, it will be monitored for one season, to prove the functionality of the system under real conditions. Simultaneously, the system acts as demonstration plant for commercial applications.

After successful demonstration of the pilot plant and its monitoring under actual conditions, the developed technology can be used for full scale testing.

An important aspect of the development is, that the production of the components is possible by Indian industry. Therefor it is planned to set up a cooperation of European and Indian industry for the production of the adsorption chiller and for the collector technology.

Literature

[1] American Society of Heating, Refrigerating and Air Conditioning Engineers (Ed.): *ASHRAE Handbook, Fundamentals*; New York, N.Y.; 1989

[2] Drück, H. and Pauschinger, Th.: *Multiport storage model for TRNSYS*; Institut für Thermodynamik und Wärmetechnik, Universität Stuttgart; Stuttgart; 1995

[3] GBU mbH: *Adsorption - Chiller TYPE NAK, 50 -430 kW*; Technical information, Bensheim, Germany

[4] Government of India (Ed.): *Country Program, Phase out of Ozone depleting substances under the Montreal Protocol*; New Delhi; September 1993

[5] Hoechst AG: *Antifrogen, Product data sheets*; Hoechst AG; Frankfurt;1996

[6] Klein, S.A., et. al.: *TRNSYS — A transient system simulation program* - Engineering Experiment Station Report 38-13; Solar Energy Laboratory; Madison-Wisconsin; 1990

[7] Khelifa N.: *Das Adsorptionspaar Silicagel-Wasserdampf, Anwendung als solares Klimatisierungssystem*; Diss.; München; 1985

[8] Köhne R., Oertel K. and Zunft, S.: *Investigation of control and simulation of solar process heat plants using a flexible test facility*; Solar Energy, Vol. 56, No. 2, pp. 169-182, 1996

[9] Mani, A.:, *Handbook of solar radiation data for India*; Allied Publishers; 1980

[10] Mani, A.:*Handbook of weather data for India*; Allied Publishers; 1990

[11] Pereira, M.C. et al.: *POSAC Project: The Potential for Solar Assisted Cooling in Southern European Countries*; Commission of The European Communities, DG12; Lisboa, Portugal; 1995

[12] Sakoda, A. and Suzuki, M.: *Fundamental Study on Solar Powered Adsorption Cooling System*; Journal of Chemical Engineering of Japan, Vol. 17, No.1; 1984

[13] N.N.: *SUNCODE-PC 5.7, A private-sector PC version of SERIRES*; Ecotope Inc., Seattle, Washington, USA

[14] Zunft, S.: *Temperature Control for Solar Process Heat Systems*; Proceedings of the ISES Solar World Congress, Budapest, 1993

Appendix A

Additional components for simulation with TRNSYS

Although TRNSYS is primarily written to describe domestic solar hot water systems most components needed are available. Only components, which describe the adsorption cooling unit and the additional heating by the genset are required. To implement the control strategy a component for a data stack is added, to stabilize the simulation.

A.1 Adsorption cooling system

A component for TRNSYS has been written, which describes the quasi stationary behavior of a two chamber adsorption cooling system. The system is modeled by the characteristic curves, taken from the technical manual of a commercial system[3] (section 5.2.1).

By these characteristic curves the effective cooling power and the coefficient of performance is evaluated for given cold water outlet, cooling water and driving temperatures. For the cold water a constant lowering of 5°C over the adsorption cooling machine is assumed, as far as it is possible due to the operation conditions. In Tab. A.1 parameters, in- and outputs are given for the TRNSYS-type.

By down-scaling of the system parameters a further mode is added by for a planned system with 15kW cooling power (`PAR(4)=2`). With the test results of methanol/silicagel experiments also the operation of a corresponding cooling system is modeled.

Parameter	Description		
1	P_{nom}	Nominal power of VAdRS: 10, 70, 170, 350 or 1050 kW	[kW]
2	$c_{p,av}$	Average specific heat capacity of heating and cooling fluid	[kJ/kg k]
3	$c_{p,c}$	Specific heat of cold water/brine	[kJ/kg k]
4	C_r	Coefficient for refrigerant: water=1 methanol=2	[-]
Input			
1	$T_{h,in}$	Heating fluid inlet temperature	[°C]
2	$\dot{m}_h$	Heating fluid mass flow	[kg/hr]
3	$T_{c,in}$	Cold water inlet temperature	[°C]
4	$\dot{m}_c$	Cold water mass flow	[kg/hr]
5	$T_{cool,in}$	Cooling water inlet temperature	[°C]
6	$\dot{m}_{cool}$	Cooling water mass flow	[kg/hr]
7	$T_{c,set}$	Cooling set temperature	[°C]
8	γ_{on}	On/off-switch (on=1)	[-]
Output			
1	$T_{h,out}$	Heating fluid outlet temperature	[°C]
2	$\dot{m}_h$	Heating fluid mass flow	[kg/hr]
3	$\dot{Q}_c$	Cooling power	[kJ/h]
4	$\dot{Q}_h$	Heating energy	[kJ/h]
5	$\dot{Q}_{aux}$	Auxiliary energy	[kJ/h]
6	$T_{c,out}$	Cold water outlet temperature	[°C]
7	$\dot{m}_c$	Cold water mass flow	[kg/hr]
8	$T_{cool,out}$	Cooling water outlet temperature	[°C]
9	$\dot{m}_c$	Cooling water mass flow	[kg/hr]
10	COP	Coefficient of performance	[-]
11	f_{Pnom}	Fraction of nominal power	[-]

Table A.1: TRNSYS component description of adsorption chiller (TYPE 78)

Parameter	Description		
1	Mode = 1-4	see TRNSYS manual	
1	Mode = 5	for power controlled operation	
2	ϵ	heat exchange effectiveness	[-]
3	$c_{p,h}$	specific heat of hot side fluid	[kJ/kg K]
4	$c_{p,c}$	specific heat of cold side fluid	[kJ/kg K]
5	UA	overall heat transfer coefficient	[kJ/hr K]
6	$\dot{m}_{h,min}$	minimum hot side mass flow	[kg/hr]
7	$\dot{m}_{h,max}$	maximum hot side mass flow	[kg/hr]
Input			
1	$T_{h,i}$	hot side inlet temperature	[°C]
2	$\dot{m}_h$	hot side fluid mass flow	[kg/hr]
3	$T_{c,i}$	cold side inlet temperature	[°C]
4	$\dot{m}_c$	cold side mass flow	[kg/hr]
5	$T_{c,set}$	cold side set temperature	[°C]
Output			
1	$T_{h,o}$	hot side outlet temperature	[°C]
2	$\dot{m}_h$	hot side mass flow	[kg/hr]
3	$T_{c,o}$	cold side outlet temperature	[°C]
4	$\dot{m}_c$	cold side mass flow	[kg/hr]
5	$\dot{Q}_T$	total heat transfer rate across heat exchanger	[kJ/hr]
6	ϵ	heat exchange effectiveness	[-]

Table A.2: TRNSYS component description of modified heat exchanger (TYPE 5)

A.2 Heat demand controlled genset

To implement the heat demand controlled genset, a special construction is used. To ensure that the heating water at the inlet of the adsorption cooling machine is always hot enough, the model of the heat exchanger (TYPE 5) for the genset exhaust is extended by mode 5 for PAR(1)=5. In this mode by INPUT(5) a set value for the fluid outlet temperature is given. With respect to the thermodynamic restrictions the energy transmission from the flue gases is controlled by the flue gas mass flow. In mode 5 constant effectiveness (PAR(2)) is taken for the heat transfer. The resulting mass flow is given as OUTPUT(2), which is limited by the minimum and maximum flue gas mass flow (PARAMETER(6) and PARAMETER(7)).

With the relation of OUTPUT(2) of the exhaust heat exchanger (UNIT 40) to the maximal flue gas mass flow the electrical power output and the mass flow of the cooling water, produced by the genset is calculated (Fig. A.1).

The cooling water mass flow defined by the flue gas mass flow of UNIT 40 is used as input for the cooling water heat exchanger (TYPE 5 / UNIT 49). This construction, the heating fluid temperature controlled genset, is modeled without

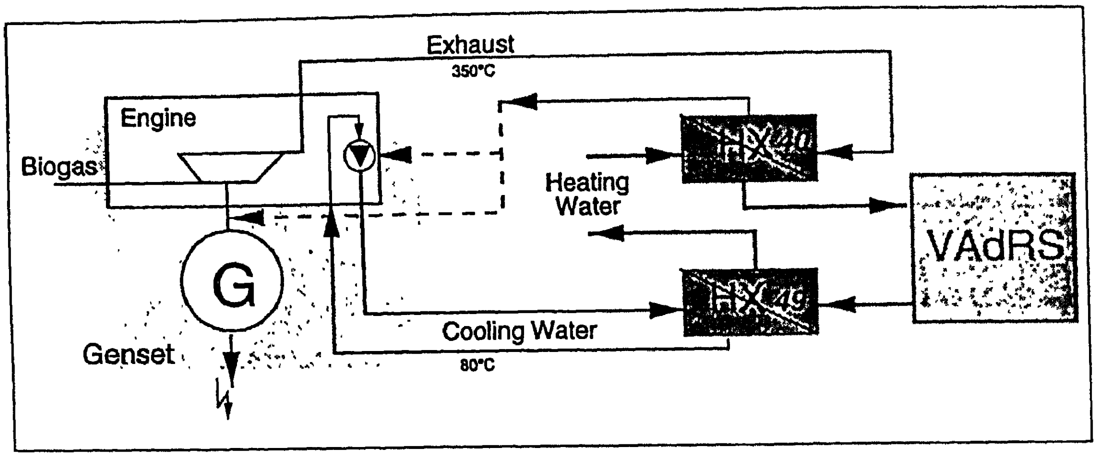


Figure A.1: Modeling of the temperature controlled genset in TRNSYS

Input	Description		
1	$x_{1,t}$	actual value of x_1	[-]
i	$x_{i,t}$	actual value of x_i	[-]
Output			
1	$x_{1,t-\Delta t}$	value of $x_1 \Delta t$ at last time step	[-]
i	$x_{i,t-\Delta t}$	value of $x_i \Delta t$ at last time step	[-]

Table A.3: TRNSYS component description of output stack (TYPE 99)

additional controller, which might cause problems during iteration in TRNSYS simulation.

A.3 Stack for the control values

The modeling of the collector outlet temperature results in several closed control loops. These would cause some problems at the simulation with TRNSYS due to the oscillating of the controlled values and thus no steady state would be found. To avoid this, the controller outputs of the last simulation time step are used for the actual control action. If the time step is small compared to the overall system behavior, the error by this small time delay can be neglected for the energy balance.

The calculations for the control are mostly implemented by EQUATION - statements in the simulation deck. As up to now there is no way in TRNSYS, to use a component output of the last time step for such an EQUATION statement, a new component (Tab. A.3) is written, which saves the output of the last time step.

A.4 Tank model

For the simulation of the preliminary model the normal TRNSYS tank module (TYPE 4) is used. During simulation however it figured out, that there is an error in the source code when modeling the boiling losses[1]. As in the preliminary concept a controlled boiler is used, to ensure the required inlet temperature for the adsorption machine, there is hardly any boiling of the heating water. Therefor this problem doesn't matter.

At the modified concept the inlet temperature is controlled by the genset exhaust heat exchanger. This causes that, for a great power supply also by the heat exchanger of the cooling water much energy is transferred. Thus the water boils frequently. Neglecting the mentioned bug would result in a high deviation of the energy balance. Therefor in modified system the multiport storage model [2] and additional pressure relief valves are used instead of TYPE 5.

[1]The boiling losses during the time step are directly added to the energy flow to the environment. Thus for time steps $\neq$1 h there is an error, as the energy loss must be added as heat flow. This bug however couldn't be fixed by the distributor.

Appendix B

TRNSYS-Simulation-Deck

The parametric study is carried out using TRNSYS 14.1 with the extensions mentioned appendix A. The modified system is described by the following deck - file.

```
*************************************************************************
* Name:india-gensetl1.dck        State 25.7.96         Kai Oertel, DLR-ITT *
*     Simulation of a solar hybrid adsorption system at New Delhi        *
*        (Output in kW)                                                   *
*            Systemparameters:                                            *
*              60 m2  CPC collector field 28.6°,                          *
*               5 m3  Buffer tank,                                        *
*              10 kW  Genset with Exhaust and cooling water HX            *
*               (load controlled)                                         *
*               5 kW  Methanonl adsoprtion chiller                        *
*                Boiling temperature 100°C                                *
*            Control parameter                                            *
*              Ton -2 °C                                                  *
*              TsollM 80°C                                                *
*              Starting condition of collector                            *
*                Eglobs 700 KJ/m2h (280W/m2)                              *
*             Starting condition of VAdRS                                 *
*                EGLOB2=1800 KJ/m2h (500W/m2)                             *
*              Pump=1800m3/h                                              *
*************************************************************************
ASSIGN year.lst            6
ASSIGN Weather/NewDehli-67.tmy 10
ASSIGN year-t.hrl          11
ASSIGN year-m.hrl          12
*ASSIGN year-e.hrl          13
ASSIGN yllc05v002gs10-e.hrl 13
ASSIGN yllc05v002gs10.sum   16
*ASSIGN year.sum            16

CONSTANTS 29
* DAY of the year of the start of the simulation
DAY = 1
* DURAtion of simulation
DURA= 300
*
TSTART = (DAY-1)*24+1
TEND   = TSTART - 1 + 24 * DURA
* TPRINT gives the timesteps for the printers of the deck
TPRINT = 1.
****************** !!!!!!!!!!! CAUTION !!!!!!!!!!! ***********************
* if TSTEP>0.01 SMOOTH can be on(=1);if TSTEP<0.01 SMOOTH should be off(=2)
* in UNIT 2 TYPE 16 SOLAR RADIATION PROCESSOR to avoid unreasonable peaks
* in solar radiation data
TSTEP  = 0.05
SMOOTH = 2
*************************************************************************
* VOLUME OF STORAGE TANK IN CUBIC METERS (M**3)
VOLUME = 2.0
*Nominal power o of the collector field in square meters (m2)
AREA = 5
* max. Powerrange PELMAX of Genset [kW] PHINFRAC minimal Load
PELMAX=10.0
* Volume of the Cold Store UNIT15/17 :Loading (100T:  * 0.8)
Vstore =80.0
* TON is the temperature which makes the ADKM to switch on in case of getting
* cold water back, that has a higher temperature than 'TON'
TON = -2
*Nominal power of the ADKM (kW)
Padkm=5
* Maximal required cooling load (kW)
MAXLOAD=3.5
* PUMDOT = mass flowrate of collector circulation pump (KG/H)
PUMDOT = 2600./1.4
* TSOLL is the temperature required to run the load circuit
TSOLLM = 80
* SLOPE of collector surfaces equals the latitude of the locality
SLOPE  = 28.6
*GTEST: mass flow per unit aperture area of the collector test (kg/(h*m2))
GTEST = 50.
*FRUl gives the slope of the efficiency curve of the collector (kJ/(h*m2*K))
* Dornier ETC : 0.79 4.9 (Tam-Tflm)/Eglob
```

```
* Solar-Prinz : 0.83 16
* Setsol CPC  : 0.74 4.0-4.2
FRUL = 4.2
* FR gives the optical efficiency of the collector
FR = 0.74
* EGLOBS gives the value of the global radiation at which pump switches on
EGLOBS = 700
* EGLOB2 makes the ADKM to get switched on whenever there is a higer radiation
EGLOB2 = 1800
*  specific heat capacity of water [kJ/kg]
CPW = 4.19
* MDOT mass flow calculated by collector modell
MCPTEST= GTEST*CPW
* min. power needed to operate plant
PELMIN=0.1
PMINFRAC=PELMIN/PELMAX
*  mass flow of ooling water and exhaust of genset at max. Power
*WATER = Pel *.3/(.4*.8*.9) /(4.19*10) * 3600 * ADKMONA
MWATERM = PELMAX *90.
MGASMAX = PELMAX * 6.8
MGASMIN = MGASMAX * PMINFRAC

SIMULATION TSTART TEND TSTEP
WIDTH 72

LIMITS 100 500 200
* iteration before warning , warnings  , calls before traces

TOLERANCES  .005 .004
*integration / convergence error (>0:relative <0: absolute)
*NOCHECK *:combined with abs. conv. error check
*DFQ 1
*DFQ solving algorithm: 1-Euler, 2-Heun, 3-Adams

NOLIST
* no listing output of the input file from here
*******************************************************************

UNIT 1 TYPE 9 CARD READER (solar radiation not interpolated)
* this is the data reader for the weather file newdelhi-67.try
PARAMETERS 14
*1mode -2:skip ,2N,3Deltat,4-6Idirnorm,7-9Itothor,10-12Tamb,13Channel,14format
    -2   4        1      -1  1  0    -2  1  0    3 0.1 0          10        0
*OUTPUTS
* 1Idirnorm, 2Itothor, 3Tamb, 19Time corresponding to values on previous line.
* 20Time corresponding to values on next line, 21 Idirnormnexthour, 22Itothor
* nexthour, 23Tambnexttimestep

UNIT 2 TYPE 16 SOLAR RADIATION PROCESSOR
* this is the radiation processor for the weather file ndelhi.dat
PARAMETERS 9
* 1mode, 2tracking, 3tiltet surface radiation mode, 4day of the year, 5latitude.
* 6solar constant, 7shift in solar time, 8smooth, 9simulation=solar time
7 1 3 DAY 28.58 4871 -2.2  SMOOTH  -1
INPUTS 9
* 1I, 2Id, 3td1, 4td2, 5Rhoground, 6Slope , 7Azimuth, 8Inext, 9Idnext
 1,2  1,1  1,19  1,20        0,0     0,0            0,0     1,22      1,21
  0     0     0     0        0.25   SLOPE             0        0         0
*OUTPUTS: 1Io, 2solarzenithangle, 3gammas, 4Itothor, 5Idiffhor, 6Itotl.
* 7Ibeamtl, 8Idifftl, 9Thetal, 10Betal

EQUATIONS 2
TAMB  = [1,3]
EGLOB = [2,6]
***************
* END WEATHER *
***************

*************************
* START CONTROLLER UNIT *
*************************
```

```
* Ein-Ausschalten mit Hysterese
EQUATIONS 4
CONTRL = GT(EGLOB,EGLOBS)*(1-[60,1])+[60,1]* GT(EGLOB,EGLOBS-300)
CONTR2 = GT(EGLOB,EGLOB2)*(1-[60,2])+[60,2]* GT(EGLOB,EGLOB2-300)
ADKMON= GT([18,1]+CONTR2,0.9)
G18=MAX([18,1],ADKMON)

UNIT 60 TYPE 99 storage of the last time step value
INPUTS 9
CONTRL CONTR2 46,2 30,2 ADKMON 30,1 26,1 32,2 20,1
   0     0      0    0    1     20   20   0   20

EQUATIONS 24
G46A   =[60,3]/PUMDOT
G26A   =[60,4]/PUMDOT
ADKMONA=[60,5]
TCOUTA =[60,6]
TPOUTA =[60,7]
G32A   =[60,8]/PUMDOT
TSPOUTA=[60,9]
* Mass flow controll (Main controll)
* MULTI: mass flow of circulation pump rised to 80% when bypass switched off
FUULL = - MCPTEST*LN(1-FRUL/MCPTEST)
MCPAF = [60,4]*CPW/MAX((AREA*FUULL),.001)
RDIM  = MCPAF * (1-EXP(-1/MAX(MCPAF,.001)))
RNOM = ((MCPTEST/FUULL)*(1-EXP(-FUULL/MCPTEST)))
R1 = MAX((RDIM/RNOM),0.9413)
ETAEGLOB = MAX( (R1*(FR*EGLOB-FRUL*(TPOUTA-TAMB)) ),0)
MDOT = MAX(0,MIN(PUMDOT,(ETAEGLOB*AREA)/MAX(.001,(CPW*(TSOLLM-TCOUTA)))))
* G26 Mass flow controller; min. massflow 9.9% with PT1-effect for stability
G26 = .5*CONTRL*MAX(MDOT/PUMDOT, .099)+.5*G26A
** Bypass regulation G32 (temperature controll) for G26<.1
*  1. Mixing temperatute
TMIX = TSOLLM+2.-TCOUTA+TPOUTA
*  2. energy balance at tee-piece no. 22
TERM1= (TMIX-TSPOUTA)/MAX(TCOUTA-TSPOUTA,0.001)
TERM = MAX(0,MIN( TERM1 ,1.))
*  3. temperature controll for G26<.1
G32 = .5*LT(G26A,.4)*(1+ADKMONA*(TERM-1) )*GT(G26A,.05)+.5*G32A
*  heat supplied by collector loop (m32/mmax<35%) or by buffer tank with second pump
*  Controll with PT1-effect for stability
G46=.5*LT((1-G32A)*G26A,.35)*ADKMONA+.5*G46A
PREMIX=MIN(1.,MAX(0.,(TMIX+2.+[50,1])/MAX(([50,1]+[10,3]),.001)))
G34=MAX(G46,PREMIX)
WATER = MWATERM*ADKMONA
EXHAU = MGASMAX*ADKMONA

UNIT 8 TYPE 2 CONTROLLER FOR BUFFER TANK
PARAMETERS 4
* 1NSTK, 2DeltaTh, 3DeltaTl, 4Tmax
     7        2          0     100
INPUTS 4
* 1Th,    2T1,  3Tin,  4Gammai
  10,12   50,3    0,0       8,1
    25     25      1          0
* OUTPUTS 1: 1Gamma0
**********************
* END CONTROLLER UNIT *
**********************

******************************
* BEGIN STORAGE OR BUFFER TANK *
******************************
UNIT 10 TYPE 4 BUFFER TANK
PARAMETERS 20
* 1Mode,     2Vt, 3Cpf, 4Rhof,  5Ut, 6H1, 7AuxMod,
       1  VOLUME  CPW   1000   1.44   -3        1
* 811,   91T1, 10Tset1, 11DeltaTdb, 12Qdotheater1,
     1     1       55           2               0
* 1312, 141T2, 15Tset2, 16DeltaTdb, 17Qdotheater2,
     1     1       55           2               0
```

```
* 18UAf, 19Tflue, 20Tboil
    0       20      120
INPUTS 5
*   1Th, 2Mdoth,     3T1, 4Mdotl,    5Tenv, 6gamma1(optional), 7gamma2(optional)
   34,3    34,4     52,3    52,4     TAMB
     25       0       25       0       20
DERIVATIVES 3
*  1T1,   2T2,   3T3
    70     70     70
*OUTPUTS 14: 1Tn, 2Mdoth, 3T1, 4Mdotl, 5Qdotenv, 6Qdots, 7DeltaE, 8Qdotaux,
* 9Qdotaux1, 10Qdotaux2, 11Qdotin, 12Taverage, 13T2, 14T3
*********************************
* END OF STORAGE OR BUFFER TANK *
*********************************

*************************
* BEGIN COLLECTOR CIRCUIT *
*************************
UNIT 20 TYPE 11 TEE-PIECE
PARAMETERS 1
1
INPUTS 4
*   1T1, 2Mdot1,    3T2, 4Mdot2
   10,1    10,2    50,1    50,2
     70       0      25       0
*OUTPUTS: 1T0, 2Mdot0

EQUATIONS 2
M20=[10,2]+[50,2]
T20=([10,1]*[10,2]+[50,1]*[50,2])/MAX(.0001,M20)+LT(M20,.0001)*[50,1]

UNIT 22 TYPE 11 TEE-PIECE
PARAMETERS 1
1
INPUTS 4
*   1T1, 2Mdot1,    3T2, 4Mdot2
    T20     M20    32,3    32,4
     70       0      25       0
*OUTPUTS: 1T0, 2Mdot0

UNIT 26 TYPE 3 PUMP FOR COLLECTOR CIRCUIT
PARAMETERS 4
* 1Mdotmax,  2Cp, 3Pmax (80W, .7bar 1.5 m3/h), 4fpar
    PUMDOT  CPW   290 .8
INPUTS 3
*   1Ti, 2Mdoti, 3gamma
   22,1    22,2     G26
     25       0       0
*OUTPUTS 3: 1To, 2Mdoto, 3P

UNIT 30 TYPE 1 FLAT-PLATE COLLECTOR
PARAMETERS 14
*1Mode, 2Ns,    3A, 4Cpc, 5Efficiency mode, 6Gtest, 7a0,  8a1. 9a2, 10epsilon.
     1    1  AREA  CPW                   2   GTEST   FR  FRUL    0          -1
*11Cpf, 12Optical mode, 13b0, 14 b1
  CPW                1   0.1     0
INPUTS 10
*   1Ti, 2Mdotc, 3Mdotf,     4Tamb,  5It,   6I,   7Id,   8rhoground, 9Theta, 10Beta
   26,1    26,2    26,2       TAMB  EGLOB  2,4    2,5          0,0      2,9    2,10
     25       0       0         20      0    0      0         0.25        0   SLOPE
*OUTPUTS 4:
* 1To, 2Mdoto, 3Qdotu, 4Tco

UNIT 32 TYPE 11 FLOW DIVERTER OF COLLECTOR BYPASS
PARAMETERS 1
2
INPUTS 3
*    1Ti, 2Mdoti, 3gamma
    30,1    30,2     G32
      25       0       0
*OUTPUTS 4: 1T1, 2Mdot1, 3T2, 4Mdot2
```

```
UNIT 34 TYPE 11 FLOW DIVERTER
PARAMETERS 1
2
INPUTS 3
*1T1,  2Mdot1, 3gamma
32,1     32,2    G34
 25        0      0
*OUTPUTS 2: 1T1, 2Mdot1, 3T2, 4Mdot2

UNIT 36 TYPE 11 TEE-PIECE
PARAMETERS 1
1
INPUTS 4
*   1T1,  2Mdot1,     3T2,   4Mdot2
   34,1     34,2     54,1     54,2
    25        0       25        0
*OUTPUTS 2: 1To, 2Mdoto

EQUATIONS 4
M54=[52,2]+[10,4]
T54=([52,1]*[52,2]+[10,3]*[10,4])/MAX(.0001,M54)+LT(M54,.0001)*[10,3]
M36=[34,2]+M54
T36=([34,1]*[34,2]+T54*M54)/MAX(.0001,M36)+LT(M36,.0001)*[34,1]

UNIT 37 TYPE 4 CAPACITY Tank
PARAMETERS 20
* 1Mode,     2Vt > Pumdot*Tstep, 3Cpf, 4Rhof,   5Ut, 6H1, 7AuxMod,
      1          .15  CPW    1000     .0    -1          1
*  811,  91T1, 10Tset1, 11DeltaTdb, 12Qdotheater1,
     1      1       55            2              0
* 1312, 141T2, 15Tset2, 16DeltaTdb, 17Qdotheater2,
     1      1       55            2              0
* 18UAf, 19Tflue, 20Tboil
      0       0      100
INPUTS 5
*   1Th, 2Mdoth,      3T1, 4Mdot1,    5Tenv, 6gamma1(optional), 7gamma2(optional)
 ' T36     M36          0,0    0,0       0,0
  25        0          25       0        20
DERIVATIVES 1
*  1T1
    70
*OUTPUTS 14: 1Tn, 2Mdoth, 3T1, 4Mdot1, 5Qdotenv, 6Qdots, 7DeltaE, 8Qdotaux,
* 9Qdotaux1, 10Qdotaux2, 11Qdotin, 12Taverage, 13T2, 14T3

UNIT 40 TYPE 5-ks HEAT EXCHANGER OF DIESEL GENERATOR EXHAUST
PARAMETERS 7
* 1Mode, 2epsilon,   3Cph, 4Cpc 5UA   6MdotHMIN   7MdothMAX
     5        0.9     1.59  CPW  30.     MGASMIN     MGASMAX
INPUTS 5
* 1Thi, 2Mdoth,    3Tci, 4Mdotc        5Tsoll
  0,0    EXHAU     37,1    37,2          0,0
  350.     0.       25.      0.          85.
*OUTPUTS 6: 1Tho, 2Mdoth, 3Tco, 4Mdotc, 5QdotT, 6Epsilon

UNIT 46 TYPE 3 MAIN CIRCULATION PUMP
PARAMETERS 4
* 1Mdotmax,   2Cp, 3Pmax (Grundfoss 40-125 1.5m3/h  7bar .6 -> 80W) , 4fpar
        PUMDOT CPW       290.       .8
INPUTS 3
*   1Ti,   2Mdoti,   3gamma
 40,3 40,4        G46
  25 PUMDOT 0
*OUTPUTS 3: 1To, 2Mdoto, 3P

EQUATIONS 2
  M47=GT(G46,.5)*[46,2]+LT(G46,.5)*[40,4]
  T47=GT(G46,.5)*[46,1]+LT(G46,.5)*[40,3]

UNIT 48 TYPE 78 ADSORPTION COOLING MACHINE
PARAMETERS 5
```

```
* 1Pnenn, 2CpmittelHeizfluid, 3CpmittelKaltfluid, 4Wasser (5Errorpr)
  Padkm      4190.                 4190.               2           0
INPUTS 8
* 1Thi, 2Mdothi,    3Tkai, 4Mdotkai, 5Tkuehli, 6Mdotkuehli, 7Tgrenz, 8Gamma
  T47      M47      14,3      14,4      0,0          0,0      TON    ADKMON
   25        0       1.         0       29.        6000.       -2       0
* OUTPUTS
* 1Tho, 2Mdotho, 3Qkalt, 4Qheiz, 5Qaux, 6Tkao, 7Mdotkao, 8Tkuehlo, 9Mdotkuehlo,

EQUATION 3
POWFRAC=[40,2]/MAX(.001,(EXHAU*EXHAU))*EXHAU
WATERS=POWFRAC*MWATERM*(1.-GT([48,1],85.))
Pel = MAX(PMINFRAC,POWFRAC)*PELMAX*3600.

UNIT 49 TYPE 5 HEAT EXCHANGER OF DIESEL GENERATOR COOLING WATER
PARAMETERS 4
* 1Mode, 2epsilon, 3Cph, 4Cpc   || 2epsilon=0:off
     4       0.9    CPW  CPW
INPUTS 4
* 1Thi, 2Mdoth,    3Tci,   4Mdotc
   0,0   WATERS     48,1     48,2
   90       0        25        0
*OUTPUTS 6: 1Tho, 2Mdoth, 3Tco, 4Mdotc, 5QdotT, 6Epsilon

*******************************************************************
* BEGIN OF STORAGE ROOM (TANK SIMULATING STORAGE CAPACITY - SEE ABOVE *
*******************************************************************
UNIT 16 TYPE 3 PUMP FOR COOLING ROOM
PARAMETERS 4
* 1Mdotmax,   2Cp, 3Pmax, 4fpar
     1700   CPW      0      0
INPUTS 3
*    1Ti, 2Mdoti, 3gamma
   48,6     48,7   18,1
      7        0       0
*OUTPUTS 3: 1To, 2Mdoto, 3P

UNIT 15 TYPE 14 Time Depending forcing function for the cooling load
PARAMETERS 20
0 0. 740 0. 1440 .93 2160 1. 2870 1. 4400 .71 5832 .48 7290 .29 7296 0. 8760 0.
*PARAMETERS 10
*0 0. 740 0. 1440 .93 2160 1. 8760 1.

UNIT 17 TYPE 14 Time Depending forcing function for the storage capacity
PARAMETERS 12
0 .3 740 .3  2160 1. 2870 1. 7290 .3  8760 .3
*PARAMETERS 8
*0 .3 740 .3  2160 1.  8760 1.

EQUATIONS 4
TONH = TON + 1.
TONL = TON + .5
* fictive massflow in kg/h, Maxload in kW, CPW in kJ/kg Vstore im m3
* here 1% of capacity
MPFIC=.01*1000.*Vstore
TFIC=[14,1]+[15,1]*MAXLOAD*3600./(CPW*MPFIC)

UNIT 14 TYPE 4 small storage tank simulating the storage room capacity
*   with variable storage capacity (XIN(8)) type4-varV
PARAMETERS 20
* 1Mode,     2Vt, 3Cpf, 4Rhof, 5Ut, 6H1, 7AuxMod
      1     Vstore  CPW   1000    0   -1         2
* 811, 91T1, 10Tset1, 11DeltaTdb1, 12Qdotheater1
    1     1      25            3              0
* 1312, 141T2, 15Tset2, 16DeltaTdb2, 17Qdotheater2
     1     1       55            5              0
* 18UAf, 19Tflue, 20Tboil,
      0      20      100
INPUTS 8
*    1Th, 2Mdoth,      3T1,   4Mdot1,   5Tenv   6gam1 7gam2 8FracCop
  TFIC     MPFIC      16,1     16,2     0,0  0,0    0,0    17,1
```

```
    0       0             7       0     TON     0.     0. 0.3
DERIVATIVES 1
*   1T1 (Anfangs: Solltemperatur Ton)
     TON
* OUTPUTS 14: 1Th, 2Mdoth, 3T1, 4Mdot1, 5Qdotenv, 6Qdots, 7DeltaE,
* 8Qdotaux, 9Qdotaux1, 10Qdotaux2, 11Qdotin, 12Taverage, 13T2, 14T3

UNIT 18 TYPE 2 CONTROLLER FOR STORAGE ROOM PUMP
PARAMETERS 4
* 1Nstk, 2DeltaTh, 3DeltaTl, 4Tmax
     7        3           1     100
INPUTS 4
*  1Th,      2T1,   3Tin,   4Gammai
  14,3       0,0     0,0         G18
   TONH      TONL       1          1
* OUTPUTS 1: 1Gamma0
**********************
* END OF STORAGE ROOM *
**********************

UNIT 50 TYPE 11 FLOW DIVERTER
PARAMETERS 1
* 1Mode
2
INPUTS 3
*  1Ti, 2Mdoti, 3Gamma
   49,3     49,4      G46
    25        0         0
* OUTPUTS 4: 1T1, 2Mdot1, 3T2, 4Mdot2

UNIT 52 TYPE 11 FLOW DIVERTER
PARAMETERS 1
* 1Mode
2
INPUTS 3
*  1Ti, 2Mdoti, 3Gamma
  50,3     50,4      8,1
   25        0         0
* OUTPUTS 4: 1T1, 2Mdot1, 3T2, 4Mdot2

UNIT 54 TYPE 11 TEE-PIECE
PARAMETERS 1
1
INPUTS 4
*    1T1, 2Mdot1,     3T2, 4Mdot2
   52,1     52,2      10,3     10,4
    25        0        25         0
* OUTPUTS 2: 1To, 2Mdoto
************************
* END COLLECTOR CIRCUIT *
************************

***********************
* START OF OUTPUT UNIT *
***********************
EQUATION 1
TPRENERGY=24

UNIT 69 TYPE 24 QUANTITY INTEGRATOR
PARAMETERS 1
* DELTA Tint
TPRENERGY
INPUTS 10
14,6 48,3 48,4 40,5 49,5 30,3 10,5 37,11 Pel 26,3
0.0  0.0  0.0   0.0  0.0  0.0 0.0  0.0   0.0  0.0

UNIT 70 TYPE 57 UNIT CONVERSION ROUTINE
PARAMETERS 30
* 3(i-1)+1: nTablei; 3(i-1)+2:Vini 3(i-1)+3:Vouti
12 1 3 12 1 3 12 1 3 12 1 3 12 1 3
12 1 3 12 1 3 12 1 3 12 1 3 12 1 3
```

```
INPUTS 10
69,1 69,2 69,3 69,4 69,5 69,6 69,7 69,8 69,9 69,10
*14,6 48,3 48,4 40,5 49,5 30,3 10,5 37,11 Pel 26,3
0.0  0.0  0.0   0.0  0.0  0.0 0.0  0.0   0.0  0.0

UNIT 71 TYPE 25 PRINTER - year-e.hrl
PARAMETERS 5
*1Deltatp,   2ton, 3toff, 4Lunit, 5UNITS
   TPRENERGY TSTART   TEND       13       2
INPUTS 10
 70,1 70,2 70,3 70,4 70,5 70,6 70,7 70,8 70,9 70,10
*14,6 48,3 48,4 40,5 49,5 30,3 10,5 37,11 Pel 26,3
 14-6 48-3 48-4 40-5 49-5 30-3 10-5 37-11 Pel 26-3
FORMAT
(F6.1,10(1x,F9.0))

UNIT 72 TYPE 25 PRINTER - year-t.hrl
PARAMETERS 5
*1Deltatp,   2ton, 3toff, 4Lunit, 5UNITS
   TPRINT  TSTART   TEND       11       2
INPUTS 10
14,12 48,6 22,1 30,1 10,12 36,1 37,1 T47 48,1 49,3
14-12 48-6 22-1 30-1 10-12 36-1 37-1 T47 48-1 49-3
FORMAT
(F6.1,10(2x,F7.2))

UNIT 73 TYPE 25 PRINTER - year-m.hrl
PARAMETERS 5
*1Deltatp,   2ton, 3toff, 4Lunit, 5UNITS
   TPRINT  TSTART   TEND       12       2
INPUTS 10
26,2  32,4 34,4 36,2 40,2 46,2 50,4 52,4 20,2 16,2
26-2  32-4 34-4 36-2 40-2 46-2 50-4 52-4 20-2 16-2
FORMAT
(F7.2,10(2x,F10.1))

EQUATIONS 1
PelPump=[46,3]+[26,3]

UNIT 74 TYPE 28    ENERGY BALANCE Total year.sum
PARAMETERS 56
*1Deltatp(-1 monthly),  2ton, 3toff, 4Lunit, 5Tablesummary
      -1    TSTART   TEND    16             2
* 6..23 Calc.-oper.
 1 0 -1 3600 2 -4 0 -1 3600 2 -4 0 -1 3600 2 -4  0 -1 3600 2 -4
   0 -1 3600 2 -4 0 -1 3600 2 -4 0 -1 3600 2 -4  0 -1 3600 2 -4
   0 -1 3600 2 -4 0 -1 3600 2 -4
INPUTS 10
*1DeltaE,2Qdcollu,3Qdenv,4Qdhxcw,5Qdhxgas 6Qdadkm 7PelPump 8Qdin37 9Pel 10Qload
10,7      30,3     10,5    49,5   40,5     48,4    PelPump  37,11   Pel   14,6
LABELS 10
DE10 Qcol Qenv10 QHXcw QHXgas QADKM PelPump Qin37  Pel Qload
CHECK 2.  -1, +2, -3, 4, 5,  -6, 7, -8

UNIT 75 TYPE 28  Solar fraction with HX 'year.sum'
PARAMETERS 28
*1Deltatp (-1 monthly),  2ton, 3toff, 4Lunit, 5Tablesummary,
 -1 TSTART TEND 16 2
*6..36 Calc.-oper.
-11 -11  -12  3 -13  3 2 -4
-14 -12 4 -13 4 -14 2 -4
-11 -15 -1 AREA 1  2  -4
INPUTS 5
* 1Qdcollu,  2Qhxcw, 3Qhxgas  4Qdotadkm 5Eglob
       30,3   49,5      40,5      48,4     EGLOB
LABELS 3
 SoFrac Deckg2  Etacoll
*********************
* END OF OUTPUT UNIT *
*********************
END
```